U.S. Department of
Transportation

**Federal Railroad
Administration**

Detection of Concrete Tie Rail Seat Deterioration

Office of Research,
Development
and Technology
Washington, DC 20590

REPORT DOCUMENTATION PAGE

Form Approved
OMB No. 0704-0188

1. AGENCY USE ONLY (Leave blank)	2. REPORT DATE September 2019	3. REPORT TYPE AND DATES COVERED Technical Report March 1, 2013 - December 31, 2016

4. TITLE AND SUBTITLE Detection of Concrete Tie Rail Seat Deterioration	5. FUNDING NUMBERS DTFR53-11-D-00008L Task Order 333
6. AUTHOR(S) Joseph LoPresti and Mike McHenry	

7. PERFORMING ORGANIZATION NAME(S) AND ADDRESS(ES) Transportation Technology Center, Inc. 55500 DOT Road Pueblo, CO 81001	8. PERFORMING ORGANIZATION REPORT NUMBER

9. SPONSORING/MONITORING AGENCY NAME(S) AND ADDRESS(ES) U.S. Department of Transportation Federal Railroad Administration Office of Railroad Policy and Development Office of Research, Development and Technology Washington, DC 20590	10. SPONSORING/MONITORING AGENCY REPORT NUMBER DOT/FRA/ORD-19/33

11. SUPPLEMENTARY NOTES
COR: Hugh Thompson

12a. DISTRIBUTION/AVAILABILITY STATEMENT This document is available to the public through the FRA website.	12b. DISTRIBUTION CODE

13. ABSTRACT (Maximum 200 words)

Rail seat deterioration (RSD) is a loss of concrete in the rail seat area of concrete ties that may compromise safety by increasing track gage, reducing fastener toe load, and allowing increased rail displacement. As part of a research project funded by the Federal Railroad Administration (FRA), and conducted by Transportation Technology Center, Inc. (TTCI), presents laboratory testing to characterize the rail and fastening system's response under loading, and in-track testing to define the conditions under which track inspection technologies can identify RSD.

Laboratory testing showed that longitudinal rail restraint decreased with increasing uniform RSD. Combined lateral and vertical loads resulted in higher lateral railhead displacements with triangular RSD than with uniform RSD. Lateral railhead displacements tended to increase with increasing amounts of triangular RSD and with increasing lateral/vertical load ratios.

In-track testing over artificial RSD test zones showed that heavy track-geometry vehicles as well as gage restraint measurement system vehicles were able to identify the triangular RSD test sections in unloaded gage and loaded gage data, respectively. Uniform RSD was not detected by either type of system. Camera-based, machine vision systems captured images that will assist in the development of imaging algorithms that may better identify RSD.

14. SUBJECT TERMS Concrete tie, rail seat deterioration, RSD, rail seat abrasion, laboratory testing, detection, inspection, gage restraint measurement system, GRMS, track geometry	15. NUMBER OF PAGES 55
	16. PRICE CODE

17. SECURITY CLASSIFICATION OF REPORT Unclassified	18. SECURITY CLASSIFICATION OF THIS PAGE Unclassified	19. SECURITY CLASSIFICATION OF ABSTRACT Unclassified	20. LIMITATION OF ABSTRACT

METRIC/ENGLISH CONVERSION FACTORS

ENGLISH TO METRIC

LENGTH (APPROXIMATE)

1 inch (in)	=	2.5 centimeters (cm)
1 foot (ft)	=	30 centimeters (cm)
1 yard (yd)	=	0.9 meter (m)
1 mile (mi)	=	1.6 kilometers (km)

AREA (APPROXIMATE)

1 square inch (sq in, in^2)	=	6.5 square centimeters (cm^2)
1 square foot (sq ft, ft^2)	=	0.09 square meter (m^2)
1 square yard (sq yd, yd^2)	=	0.8 square meter (m^2)
1 square mile (sq mi, mi^2)	=	2.6 square kilometers (km^2)
1 acre = 0.4 hectare (he)	=	4,000 square meters (m^2)

MASS - WEIGHT (APPROXIMATE)

1 ounce (oz)	=	28 grams (gm)
1 pound (lb)	=	0.45 kilogram (kg)
1 short ton = 2,000 pounds (lb)	=	0.9 tonne (t)

VOLUME (APPROXIMATE)

1 teaspoon (tsp)	=	5 milliliters (ml)
1 tablespoon (tbsp)	=	15 milliliters (ml)
1 fluid ounce (fl oz)	=	30 milliliters (ml)
1 cup (c)	=	0.24 liter (l)
1 pint (pt)	=	0.47 liter (l)
1 quart (qt)	=	0.96 liter (l)
1 gallon (gal)	=	3.8 liters (l)
1 cubic foot (cu ft, ft^3)	=	0.03 cubic meter (m^3)
1 cubic yard (cu yd, yd^3)	=	0.76 cubic meter (m^3)

TEMPERATURE (EXACT)

[(x-32)(5/9)] °F = y °C

METRIC TO ENGLISH

LENGTH (APPROXIMATE)

1 millimeter (mm)	=	0.04 inch (in)
1 centimeter (cm)	=	0.4 inch (in)
1 meter (m)	=	3.3 feet (ft)
1 meter (m)	=	1.1 yards (yd)
1 kilometer (km)	=	0.6 mile (mi)

AREA (APPROXIMATE)

1 square centimeter (cm^2)	=	0.16 square inch (sq in, in^2)
1 square meter (m^2)	=	1.2 square yards (sq yd, yd^2)
1 square kilometer (km^2)	=	0.4 square mile (sq mi, mi^2)
10,000 square meters (m^2)	=	1 hectare (ha) = 2.5 acres

MASS - WEIGHT (APPROXIMATE)

1 gram (gm)	=	0.036 ounce (oz)
1 kilogram (kg)	=	2.2 pounds (lb)
1 tonne (t)	=	1,000 kilograms (kg)
	=	1.1 short tons

VOLUME (APPROXIMATE)

1 milliliter (ml)	=	0.03 fluid ounce (fl oz)
1 liter (l)	=	2.1 pints (pt)
1 liter (l)	=	1.06 quarts (qt)
1 liter (l)	=	0.26 gallon (gal)
1 cubic meter (m^3)	=	36 cubic feet (cu ft, ft^3)
1 cubic meter (m^3)	=	1.3 cubic yards (cu yd, yd^3)

TEMPERATURE (EXACT)

[(9/5) y + 32] °C = x °F

QUICK INCH - CENTIMETER LENGTH CONVERSION

	0	1	2	3	4	5

Inches

Centimeters

| 0 | 1 | 2 | 3 | 4 | 5 | 6 | 7 | 8 | 9 | 10 | 11 | 12 | 13 |
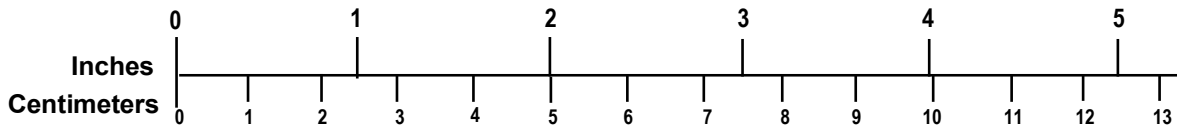
QUICK FAHRENHEIT - CELSIUS TEMPERATURE CONVERSION

°F	-40°	-22°	-4°	14°	32°	50°	68°	86°	104°	122°	140°	158°	176°	194°	212°
°C	-40°	-30°	-20°	-10°	0°	10°	20°	30°	40°	50°	60°	70°	80°	90°	100°
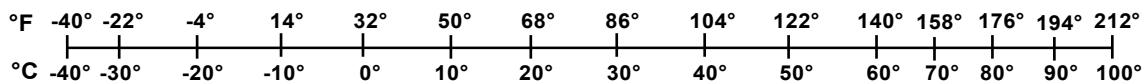
For more exact and or other conversion factors, see NIST Miscellaneous Publication 286, Units of Weights and Measures. Price $2.50 SD Catalog No. C13 10286

Acknowledgements

Contents

Illustrations

Tables

Executive Summary

Rail seat deterioration (RSD) is a documented failure mode of concrete ties exhibited by degradation of the concrete surface that supports the rail. Multiple derailments of both passenger and freight trains were attributed to RSD. RSD is difficult to detect visually during traditional walking or hi-rail track inspections.

Transportation Technology Center, Inc. (TTCI) performed laboratory and in-track testing at the Transportation Technology Center to better understand the detection of RSD on concrete ties in three phases from March 1, 2013, through December 31, 2016. This study, funded by the Federal Railroad Administration (FRA), examined how the rail, in the presence of RSD, behaved under loading and how to best detect various magnitudes and types of RSD. The project included three primary parts:

1. Accumulation of tonnage at the Facility for Accelerated Service Testing (FAST) on ties with and without preexisting RSD

2. Laboratory testing to characterize rail behavior in the presence of RSD

3. Development of an RSD test facility and detection system testing

Phase I involved installing concrete ties with and without preexisting artificial (ground in) RSD at the High Tonnage Loop (HTL) at FAST. No significant additional RSD was developed. This corroborated historical evidence that RSD has not been a typical failure mode at FAST, and that the loads produced by the FAST train were not sufficient to result in RSD in the absence of other factors, such as persistently wet conditions or poor track geometry.

Phase II included laboratory testing on concrete tie rail seats with various types and magnitudes of RSD. Rail longitudinal restraint, clip toe load, and rail lateral/vertical compliance tests were conducted using American Railway Engineering Maintenance-of-Way Association's (AREMA) *Manual for Railway Engineering* test procedures as guidance. Longitudinal restraint generally decreased with increasing uniform RSD; the effect of increasing triangular RSD was less pronounced. Ties with uniform RSD exhibited reduced toe loads on both clips while ties with triangular RSD exhibited reduced toe load on only the field side clip, corresponding with the depth of deterioration. Higher magnitudes of triangular RSD resulted in higher lateral railhead displacements while increasing depths of uniform RSD did not appear to affect railhead lateral displacements to the same degree.

Phase III involved the development of an RSD test facility at FAST. Four test zones were established using concrete ties with artificial RSD of various types and magnitudes. Industry vendors of track inspection and measurement systems were invited to participate in the study. Data from track geometry vehicles, gage restraint measurement systems (GRMS), and a machine vision system were analyzed. Generally, track geometry and GRMS vehicles were able to detect the presence of triangular RSD, but not uniform RSD, in the gage and loaded gage channels respectively. Higher applied lateral/vertical load ratios increased the visibility of the RSD in the loaded gage channel of GRMS system. The machine vision system tested did not have an algorithm established to automatically detect RSD, however images collected during testing clearly indicate RSD and may be used to develop such an algorithm.

Overall, results suggest that the most robust method of detecting RSD may be the combination and overlay of multiple techniques. While GRMS and track geometry channels can indicate RSD, a machine vision system may augment the inspection process and reduce the occurrence of false-positive (or false negative) outputs.

1. Introduction

Rail seat deterioration (RSD) of concrete ties is manifested by the loss of concrete tie material under the rail seat area and, in extreme cases, can result in loss of rail clip holding power (toe load), negative (outward) rail cant, gage widening, and rail rollover [1]. Figure 1 shows an example of RSD.

Figure 1. Rail Seat Deterioration

The Federal Railroad Administration (FRA) contracted with Transportation Technology Center, Inc. (TTCI) to investigate RSD. This report describes research conducted under Phase III of a broader FRA-funded investigation of RSD—a study to better understand the inspection for and detection of RSD.

During Phase I of the investigation, concrete ties were inspected and measured in 16 curves on 2 railroads, encompassing a range of environmental conditions and track curvature [2]. For a few of the measured curves, RSD measurements were compared to measured track geometry and wheel-rail forces generated by NUCARS®[1] simulations to correlate wheel-rail forces and deterioration depth. The NUCARS simulations confirmed a correlation of RSD with track curvature, but could not identify specific track geometry features associated with severe RSD [2].

During Phase II, TTCI completed NUCARS track model simulations to examine the effects of combination track geometry deviations on rail seat stresses and the generation of RSD [3]. Additionally, an in-track test section was installed at the Facility for Accelerated Service Testing (FAST) to verify model simulation results. Results from Phase II indicated that various track geometry perturbations, e.g., loss of superelevation in combination with poor alignment within FRA Class 4 limits, can produce higher stresses at the rail seat. However, loads generated in the worst-case simulations and in-track geometry deviations do not exceed the typical compressive strength of concrete. Overall, the results of this phase augment support for an abrasive mechanism for RSD, related to fines and moisture intrusion in the rail seat and not to ultimate compressive failure of the concrete [3].

---

[1] NUCARS® is a registered trademark of TTCI in Pueblo, CO.

Phase III of the broader RSD investigation, and the topic of this report, focused on the response of the track to RSD and how best to detect existing RSD in-track. It included three primary parts outlined in the study approach below.

This report details the results of these three parts of the project and provides recommendations, on the basis of these results, on improved detection of RSD during track inspections. Conclusions from this report augment findings from the first two phases of the broader RSD study to provide an overall better understanding of the mechanisms for RSD, the loading environment of the rail seat, and the detection of RSD in-track.

1.1   Background

As concrete ties have been more widely adopted, researchers continually work to better understand their performance and failure modes [1] [8]. Concrete ties exhibited cracking, reinforcement delamination, and RSD. Recent derailments were attributed to RSD where concrete ties in curves exhibited large, wedge-shaped loss of material on the field side of the rail seat area [4]. This failure mode contributed to increased gage widening under passing wheel loads and, in combination with reduced fastener toe load, increased rail rollover.

Two distinct modes of RSD were identified: uniform (also termed vertical) and triangular, as Figure 2 shows.

(a)   (b)
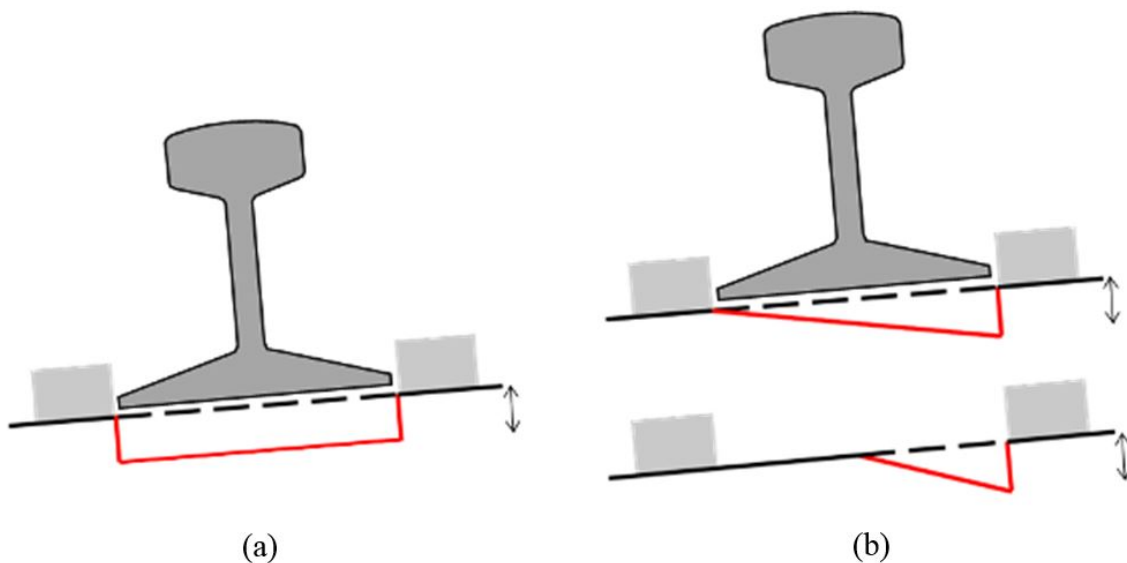
**Figure 2. Two Distinct Modes of RSD—(a) Uniform and (b) Triangular,
Including Half-Triangular**

Uniform deterioration is generally more consistent in depth across the rail seat area, and associated with tangent track. The triangular mode results in wedge-shaped deterioration, with more deterioration toward the field side of the rail seat. The deterioration may affect all, or only a portion of, the rail seat area. The latter, termed "half-triangular," is a type of RSD included in the study after discussions between the TTCI research team and researchers from Volpe National Transportation Systems Center (Volpe). Triangular RSD is typically associated with curves where higher applied lateral loads can generate higher stresses on the field side of the high rail

seat [2]. There were derailments on Class I railroads attributed to RSD [3]. Preliminary modeling studies conducted by Volpe suggested that once RSD had initiated, it might excite vehicle dynamics that could increase forces acting on the rail seat [5]. The same research also indicated that these increased forces might be high enough to exceed the compressive strength of concrete and exacerbate the development of RSD. Recent testing showed increased rail seat forces caused by existing RSD, but not high enough to exceed typical concrete compressive strengths [7]. The rate at which RSD develops is not as well documented, but anecdotal reports suggest that RSD can progress rapidly once initiated. The rate of RSD progression is important to consider when discussing inspection techniques and frequencies.

Since evidence of RSD is often obscured by the rail, rail pad, and fasteners, it can be difficult to detect during conventional walking or hi-rail track inspections, typically conducted by viewing the track down its centerline and not in detail at each rail seat. As high speed and high tonnage traffic is often moved on concrete tie track corridors, improved methods of inspecting concrete ties for RSD are desirable to improve the safety and efficiency of operations.

1.2 Objectives

The objective of this study was to better understand the behavior of rail in the presence of RSD with specific attention to the inspection for and detection of concrete tie RSD.

1.3 Overall Approach

The approach for this study included three phases:

1. An accumulation of tonnage at FAST on preexisting RSD.
2. Laboratory testing to characterize rail behavior in presence of RSD.
3. The development of an RSD test facility and detection system testing.

Phase I involved installing concrete ties with and without preexisting artificial (ground in) RSD in a test curve at the High Tonnage Loop (HTL) at the FAST. RSD has historically not been observed at FAST. The objective of this portion of the test was to determine if preexisting RSD would exacerbate rail seat loads and generate increased RSD as tonnage was accumulated. The rate of RSD development is important in determining the frequency and detail of track inspections in concrete tie territories.

Phase II included laboratory testing on concrete tie rail seats with various types and magnitudes of RSD. Rail longitudinal restraint, clip toe load, and rail lateral/vertical compliance tests were conducted using AREMA *Manual for Railway Engineering* test procedures as guidance. These tests were performed to provide indications of anticipated rail movement during track loading under various types and magnitudes of RSD.

Phase III involved the development of an RSD test facility at FAST. Four test zones were established in a test section of track using concrete ties with artificial RSD of various types and magnitudes. Industry vendors of track inspection and measurement systems were invited to participate in the study by testing over these zones and sharing data with TTCI. Data from track geometry vehicles, gage restraint measurement systems (GRMS), and a machine vision system were analyzed.

1.4   Scope

The purpose of this project is to better understand how existing RSD can be detected in-track and how rapidly it may develop. This project was composed of three primary tasks—laboratory testing, in-track testing at FAST, and RSD detection testing using various inspection vehicles and systems. The lab testing was conducted to increase understanding of rail responses under load in the presence of RSD, and to identify rail responses that could be indicators of RSD. The in-track testing at FAST accumulated tonnage on concrete ties with and without pre-existing RSD to document how the RSD developed as tonnage was accumulated in a Heavy Axle Load (HAL) environment. Lastly, an artificial RSD test section was installed on a siding track as a test bed to evaluate how various track inspection vehicles and systems can identify four different types and magnitudes RSD.

1.5   Organization of the Report

This report was comprised of five sections where Section 1 provides an introduction of the project, Section 2 discusses the in-track testing at FAST, Section 3 analyzes the laboratory testing, Section 4 also analyzes the in-track detection testing, and Section 5 offers a conclusion along with recommendations for future work.

2. In-Track Testing at FAST—Ties with and without Preexisting RSD

To better understand the mechanisms and development of RSD under heavy axle load traffic, ties with and without preexisting RSD were installed at FAST and monitored for 375 million gross tons (MGT) of accumulation.

FAST is a part of the Association of American Railroads (AAR) Strategic Research Initiative (SRI) program. An 18,000-ton train, consisting of cars predominately loaded to 315,000 pounds, is operated on the HTL where the performance of track components and structures is evaluated under the heavy axle load train. Test ties were installed in a 5-degree curve with 4 inches of superelevation. With a standard operating speed of 40 mph resulting in an overbalanced condition (curve is balanced at 33 mph), the high rail of the curve is loaded more severely than the low rail. The climate at the Transportation Technology Center (TTC), located on the high plains northeast of Pueblo, CO, is fairly arid with average precipitation averaging less than 12 inches per year. It was desirable to determine the rate at which RSD would progress in this load environment, particularly for the ties with preexisting RSD. The rate of RSD progression is important to consider when planning the frequency and detail of inspections.

Twelve test ties were installed in the 5-degree curve. Eight of the 12 ties were ground to simulate full triangular RSD in a manner similar to the ties tested in the laboratory. The depth of grinding at the field-side shoulder of the ties ranged from 0.625 inch to 0.25 inch with the center two ties having the deepest grinding. The 2 ties at each end of the 12 were not ground. The 12 test ties were Con-Force Costain CN 60C designs with e-clip shoulders. Figure 3 shows the eight ground rail seats before the ties were installed at FAST. Figure 4 shows a detailed view of a rail seat ground with 0.1875-inch depth of triangular RSD.

**Figure 3. Rail Seats Ground to Simulate Triangular RSD
before Installation at FAST (0 MGT)**

7

Figure 4. Detailed View of Ground Rail Seat with 0.1875-inch triangular RSD before installation at FAST

The condition of the ties was photo documented before the ties were installed, and when the ties were removed after accumulating 375 MGT. Figure 5 shows photos of two rail seats after 375 MGT—one that had not been ground at 0 MGT (Figure 5a), and one that initially had 0.25-inch of triangular RSD ground in (Figure 5b).

Figure 5. Rail Seats from the FAST installation. (a) Unground Rail Seat after 375 MGT, and (b) Tie with 0.25-inch Ground Rail Seat after 375 MGT

The surface conditions of the ground and unground ties before and after the test were similar. To quantify material loss, depth measurements of the rail seats were taken before and after tonnage accumulation. Depth measurements were taken at 32 different locations along the width of the rail seat (from shoulder to shoulder along the length of the tie) using a linear variable displacement transducer (LVDT) and a custom depth gage fixture shown in Figure 6.

Figure 6. RSD Depth Measurement Gage used to Measure RSD of Ties Installed at FAST at 0 MGT and 375 MGT

All 12 test ties, whether ground or unground, exhibited only minor material loss and RSD. Figure 7 shows rail seat profiles measured at 0 and 375 MGT for two ties—one that was not ground, and one that was ground to a depth of 0.25-inch on the field side. The slope of the ground rail seat is steeper on the field side than it is on the gage side. There was some variability in the grinding, as there is in actual RSD. Each series represents a depth profile across the width of the rail seat.
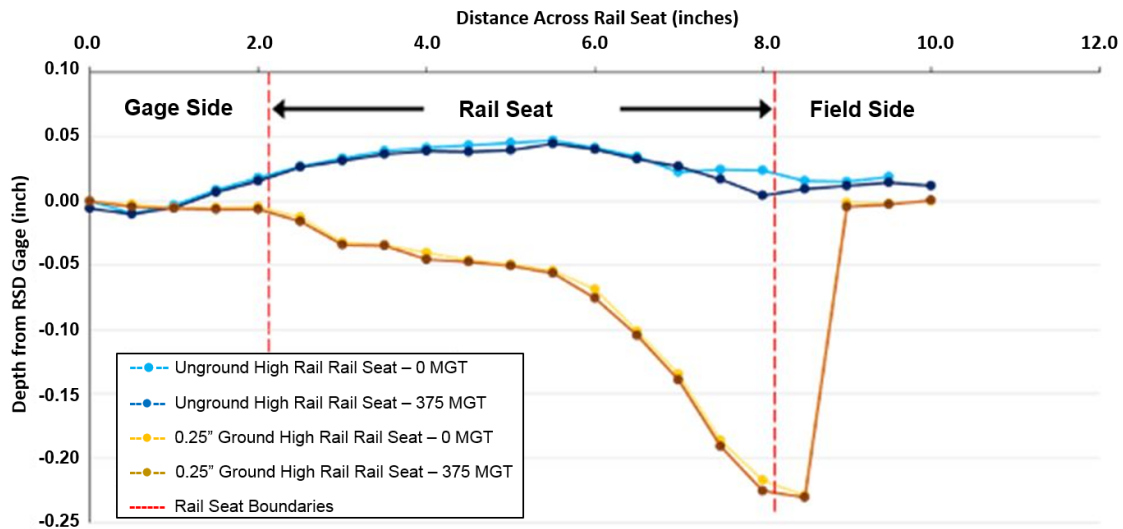
Figure 7. Transverse Profiles across Two Rail Seats at 0 MGT and 375 MGT of Accumulated Tonnage at FAST

9

The maximum change in depth measured after 375 MGT was less than 0.02 inch, and the changes in measured depths were similar for the tie that was not ground and for the tie that was ground, indicating insignificant development of RSD or RSD growth. Results were similar for the other 10 ties in the test zone. This result aligns with previous observations at FAST, namely, that RSD has not presented itself as a typical failure mode of concrete ties in the loading environment at FAST. Moreover, as installed, the presence of preexisting RSD did not appear to initiate additional degradation of the rail seat. Moisture on the rail seat has been purported to accelerate the development of RSD. With the arid climate in Pueblo, CO, this study (and historical observations) appear to confirm that moister environments are more conducive to RSD development than the overbalanced speed and high lateral loads characteristic of FAST operations in a dry environment. In addition, the ties, shoulders, and concrete were in good condition when installed at FAST. Ties that had weathered or were produced with lower strength concrete might have performed differently. The effect of concrete quality control in the concrete tie manufacturing process on RSD development is not clear.

3. Laboratory Testing

Before in-track inspection testing, preliminary laboratory testing was conducted to better understand anticipated rail behavior in the presence of RSD. Test ties were prepared with varying magnitudes and types of RSD. The following three tests were performed on each tie:

1. Rail longitudinal restraint
2. Rail uplift/clip toe load
3. Lateral/vertical rail compliance

This testing demonstrated rail roll and deflections under combined vertical and lateral load as well as the effect of RSD on toe load and rail longitudinal restraint. Results were used to better understand how RSD might be detected in track.

3.1 Preparation of Test Ties

Concrete test ties with embedded PANDROL® SAFELOK I shoulders were selected. Figure 8 shows that full-length concrete ties were cut into 22-inch sections that included the rail seat (two rail seats per tie). Nine concrete tie samples were prepared and their rail seats were ground to simulate the various types and magnitudes of RSD. Four concrete ties were prepared with uniform RSD (0.125-inch, 0.25-inch, 0.375-inch, and 0.5-inch depths), Figure 9 and Figure 10, and four concrete ties were prepared with triangular RSD (0.25-inch, 0.5-inch, 0.75-inch, and 1-inch depths on the field side), Figure 11 and Figure 12, and one concrete tie had no RSD. One wood tie was also prepared as shown in Figure 13, with cut spikes and rail anchors to provide a comparison.

New fastener assemblies (PANDROL® SAFELOK I clips, insulators, and tie pads) were used for each test configuration. The same 10 tie sections were used throughout the testing.
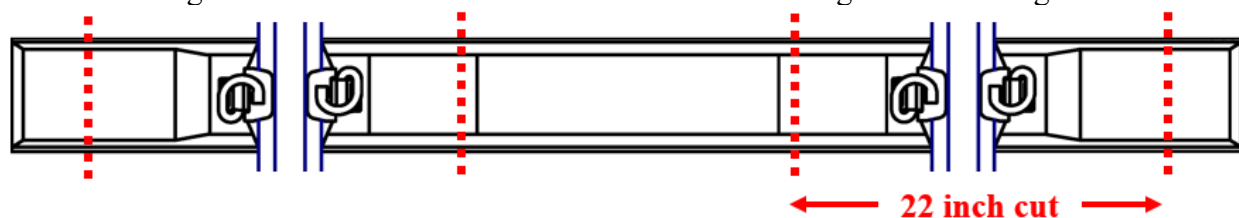
Figure 8. Tie Cutting for Laboratory Testing

Figure 9. Example of Concrete Tie Section with Uniform RSD

Figure 10. Example Showing Uniform RSD Depth Profile

Figure 11. Example of Concrete Tie Section with Triangular RSD

Figure 12. Example Showing Triangular RSD Depth Profile
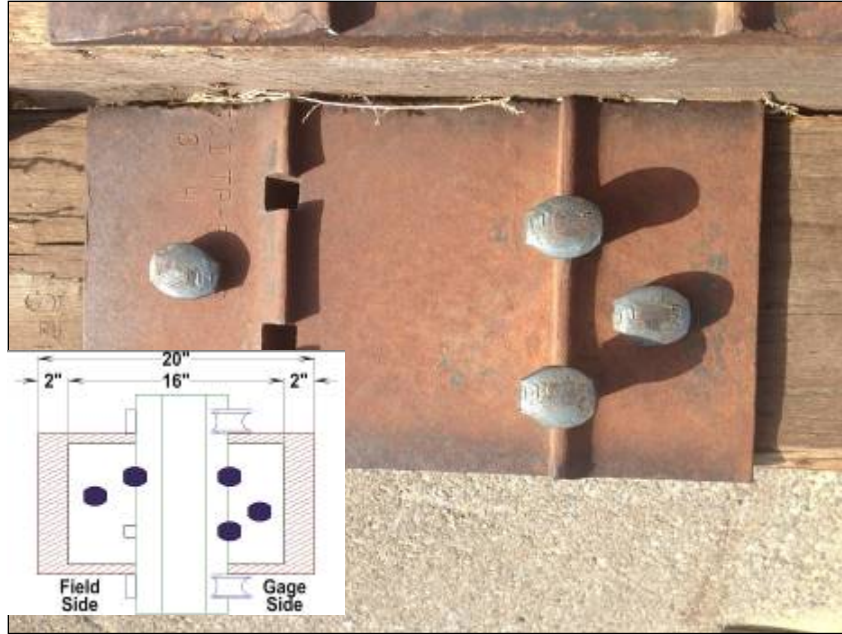
Figure 13. Spiking Pattern for Wood Tie with 16-inch Six-Hole AREMA Tie Plate with Two Gage Side Rail Spikes (Inset-Field Side Rail Spike Added after Fixture Attachment)

3.2   Laboratory Test Equipment

Laboratory testing was conducted on TTCI's Three-Post Load Frame. The load frame consists of a 50,000-pound vertical servo-controlled MTS actuator and controller (Figure 14). The actuator has an integrated load cell and LVDT. Custom fixtures were constructed for each test to provide sufficient restraint of the tie sections. Additional LVDTs were also used to measure rail displacements as indicated. All testing was conducted at ambient room temperature (70 °F +/-10 °F).

Figure 14. Three-Post Load Frame

The procedures for each of the three laboratory tests are described in the following sections.

3.3 Rail Longitudinal Restraint

The longitudinal restraint test measures the longitudinal restraint of the rail provided by the fastening system. The tests were performed in accordance with AREMA Chapter 30 Test 5B recommended practices [9]. The effect of RSD on rail longitudinal restraint was determined by performing the same test procedure on all nine concrete tie sections. Additionally, results were compared with those for the wood tie and cut spike fastening system where the longitudinal restraint is provided by rail anchors.

3.3.1 Test Procedure

Figure 15 shows a schematic of the test setup [9]. Figure 16 shows a picture of the test setup and fixture used to restrain the tie section.
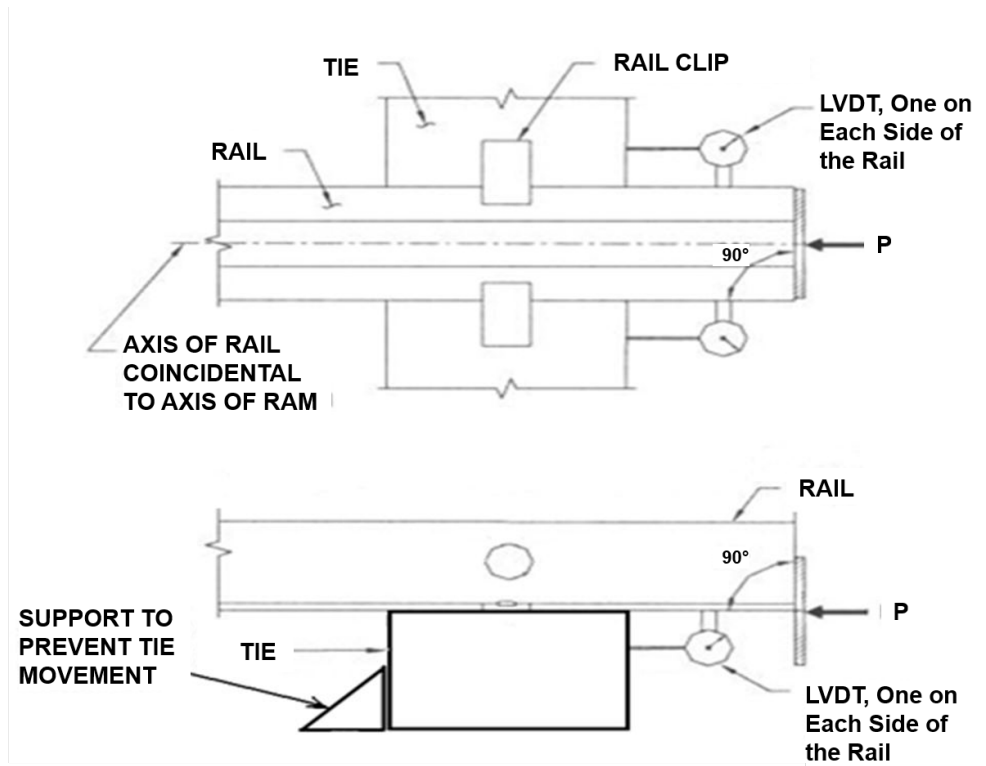
Figure 15. Rail Longitudinal Restraint Test Setup [9]

Figure 16. Rail Longitudinal Restraint Fixture

The tie section was fastened to the base of the fixture, and a short length of 136RE rail base was clipped to the tie using the SAFELOK I fastening system components and recommended installation procedure. The following instrumentation channels were collected:

1. Longitudinal applied load
2. Longitudinal displacement (in-line actuator LVDT)
3. Left side longitudinal rail displacement
4. Right side longitudinal rail displacement
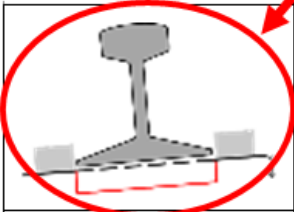
Longitudinal load was applied to the rail section in increments of 400 pounds. Longitudinal rail displacement was recorded at each increment. The test continued until a load of 2,400 pounds was reached or until longitudinal rail displacement exceeded 0.5 inch. If the load reached 2,400 pounds with less than 0.5 inch of displacement, 2,400 pounds was held for 15 minutes, as recommended by the AREMA test procedure.

3.3.2 Results

AREMA recommends that the maximum longitudinal rail displacement throughout the loading increments, or during the holding of 2,400 pounds of longitudinal force, not to exceed 0.20 inch. However, it was observed during testing that there was an obvious "break-free force" at which the longitudinal displacements quickly exceeded 0.20 inch. The in-line LVDT of the actuator was found to produce more consistent and accurate longitudinal rail displacements, so this channel was used in lieu of the two rail-mounted LVDTs.

Table 1 displays the longitudinal force increment at which the rail broke free.

Table 1. Longitudinal Break Free Force

	Tie Type	Break Free Force Increment (pounds)
	Wood Tie/cut spikes and rail anchors	Did not break free
	Concrete Zero RSD	Did not break free
	Concrete 0.125-inch Uniform RSD	2,400
	Concrete 0.25-inch Uniform RSD	1,600
	Concrete 0.375-inch Uniform RSD	1,200
	Concrete 0.5-inch Uniform RSD	800
	Concrete 0.25-inch Triangular RSD	2,400
	Concrete 0.5-inch Triangular RSD	2,400
	Concrete 0.75-inch Triangular RSD	2,400
	Concrete 1-inch Triangular RSD	2,400

Results in Table 1 clearly show that as uniform RSD magnitude increased, the longitudinal rail restraint provided by the tie and fastener system decreased. Longitudinal restraint in a concrete

17

tie fastening system is provided by the friction between the rail and clips, the rail and the rail pad, and rail pad and concrete rail seat. Increased clip toe load serves to increase the normal force acting through these frictional interactions, correspondingly increasing the longitudinal restraint provided.

As expected, the wood tie and non-deteriorated concrete tie rail seat did not exhibit any excessive displacement throughout the loading increments or during the holding of the 2,400-pound load. All magnitudes of triangular RSD produced excessive longitudinal rail displacements at the 2,400-pound loading increment. However, increased triangular RSD magnitude does not appear to affect the longitudinal restraint provided by the fastening system. This suggests that the non-deteriorated gage side of the rail seat (and corresponding gage side clip) contributed similar longitudinal restraint for each of the triangular RSD test cases, regardless of the depth of the RSD. If both sides of the rail seat are deteriorated (as in the case of uniform RSD), reducing the toe load of both the gage side and field side clip toe loads, the longitudinal restraint appears to be more significantly affected.

3.4   Vertical Rail Uplift (Toe Load) Test

The vertical rail uplift test measures the applied load and displacement of the rail as it is lifted vertically. Results from this test provide an indication of the fastener toe load being provided. The effect of the various types and magnitudes of RSD on clip toe load was compared.

3.4.1   Test Procedure

Figure 17 shows a schematic of the test setup. Figure 18 shows a photo of the test setup and fixture used to restrain the tie section. For this test, a single tie section was fastened to the test fixture and a short length of 136RE rail was clipped to the tie using standard SAFELOK I fastening system components and manufacturer recommended installation procedures. The rail fixture used had a 1.5-inch diameter hole drilled in the web. The rail was connected to the actuator with a shear pin and clevis, as Figure 17 shows.
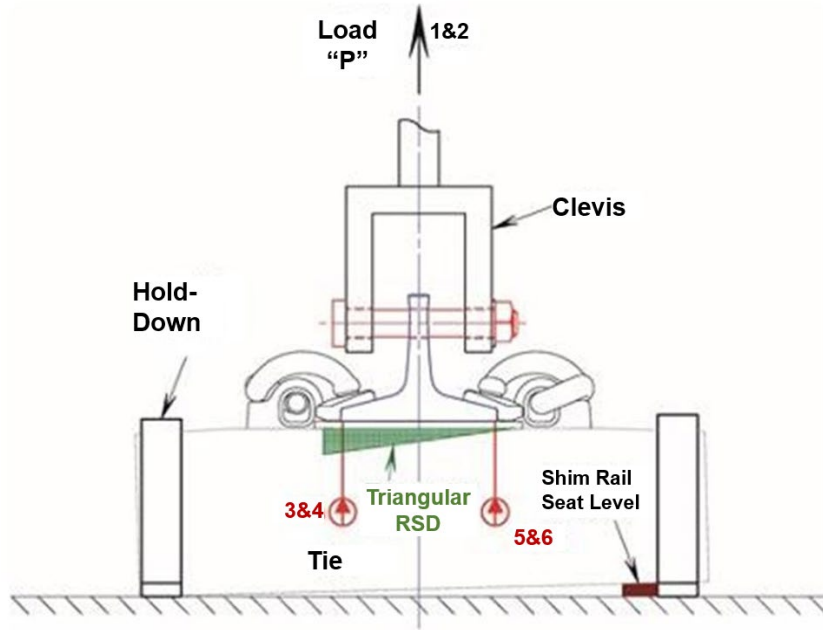
Figure 17. Test Assembly and Load Application (Shown for Triangular RSD)

Figure 18. Vertical Rail Uplift Fixture

The test procedure was guided by AREMA Test 5B [9]. An uplift (tensile) load was applied at a rate of 1,000 pounds per minute to the system until 6,000 pounds was reached, then the system was unloaded. The following channels were collected throughout the test.

1. Vertical applied load
2. Vertical displacement (in-line actuator LVDT)
3. Left side field side vertical rail displacement
4. Left side gage side vertical rail displacement
5. Right side field side vertical rail displacement
6. Right side gage side vertical rail displacement

AREMA recommended practice states that the load required to lift the rail base 0.05 inch from its initial position is designated as the toe load. The test sequence was repeated once for each configuration.

3.4.2 Results

Figure 19, Figure 20, and Figure 21 show the applied tensile load versus rail vertical displacement curves for the non-deteriorated concrete tie, 0.125-inch uniform RSD, and 0.5-inch uniform RSD cases, respectively. The hysteresis after unloading is shown for each case.
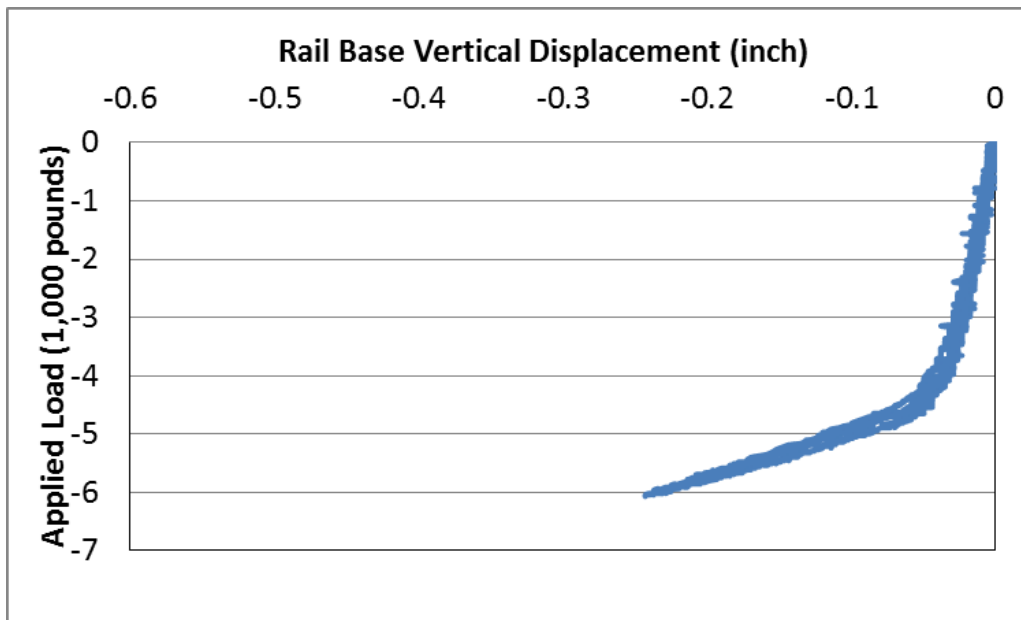
Figure 19. Load vs. Vertical Displacement Curve for Concrete Tie Zero RSD
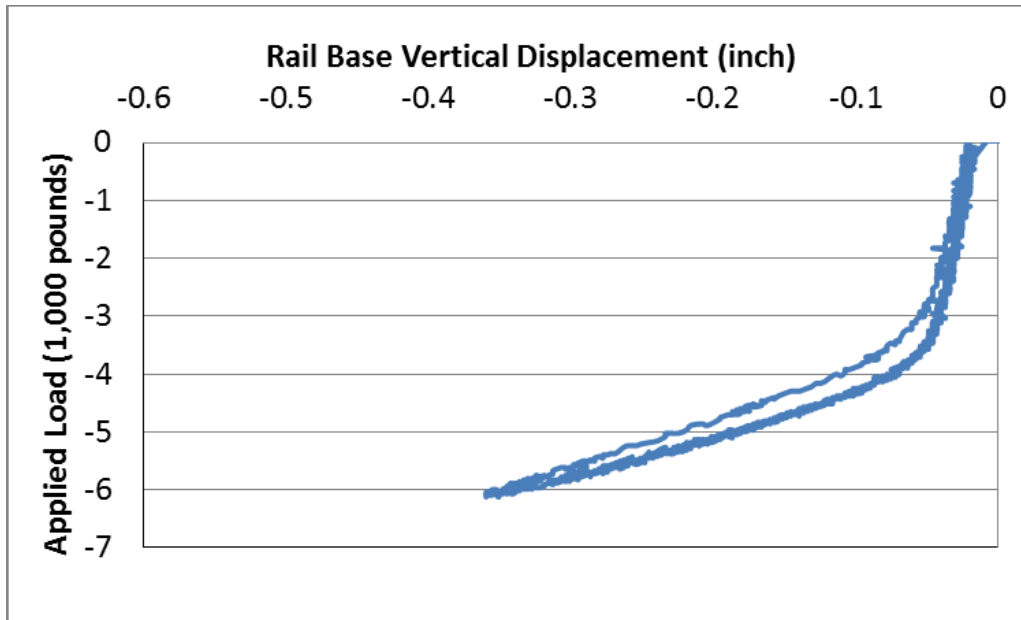
Figure 20. Load vs. Displacement for Concrete 0.125-inch Uniform RSD
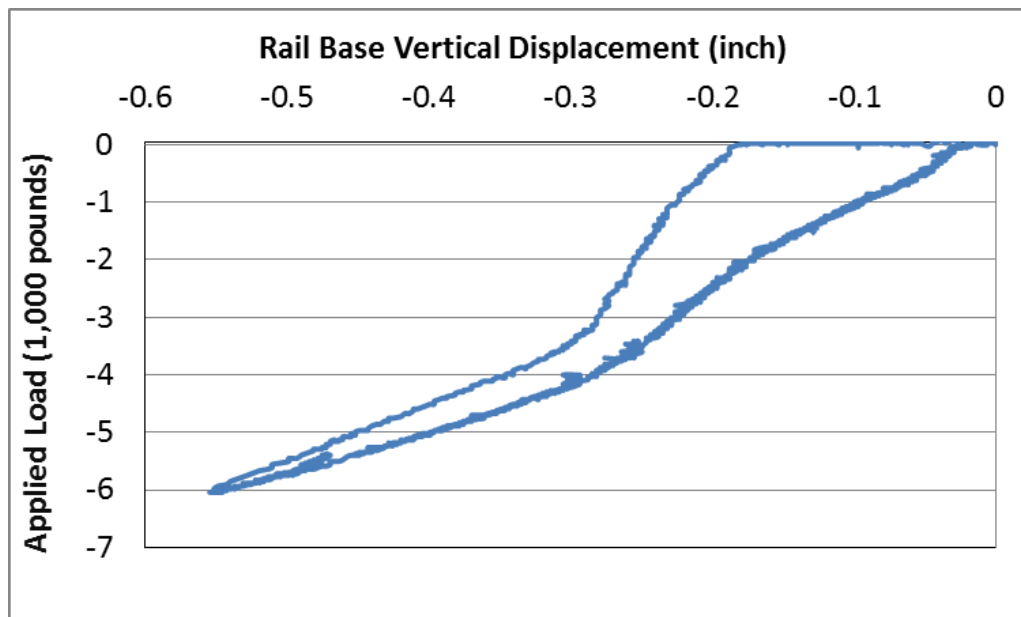
Figure 21. Load vs. Displacement for Concrete 0.5-inch Uniform RSD

Results suggest that as uniform RSD magnitude increases, the clip toe load decreases. Higher magnitudes of uniform RSD resulted in lower uplift forces required to reach the AREMA defined threshold of 0.05 inch of vertical displacement.

Results from the triangular RSD concrete ties were inconclusive, as vertical displacements on the gage and field side varied. Since the load is applied at the rail web, triangular RSD tended to introduce an eccentricity that caused rail rotation as well as uplift. As expected for triangular

RSD cases, it was observed that the gage side clip produced a higher toe load than the field side clip. This observation is in line with results from the longitudinal rail restraint test.

3.5 Lateral/Vertical Compliance

Lateral/vertical compliance testing was conducted to measure rail rotation and deflection under a combined vertical and lateral load. The effect of the various types and magnitudes of RSD on rail behavior was measured under a variety of lateral/vertical (L/V) load ratios. This test assessed the compliance of the tie and fastener system under different severities of gage widening loads, such as those applied in-track with GRMS vehicles, a common technique for inspecting track for RSD.

3.5.1 Test Procedure

Figure 22 shows a schematic of the test setup for triangular RSD. Figure 23 shows a photo of the test setup and fixture used to restrain the tie section.
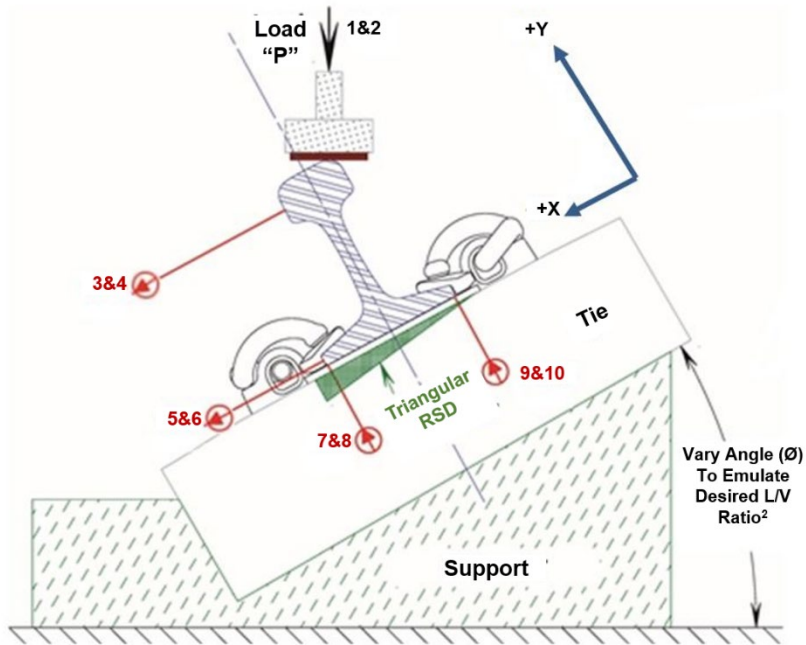
Figure 22. Lateral/Vertical Compliance Test Setup (Shown for Triangular RSD)

Figure 23. Lateral/Vertical Compliance Fixture

For this test, a single tie section was fastened to the test fixture and a short length (approximately 1 foot) of 136RE rail was clipped to the tie using standard SAFELOK I fastening system components and manufacturer recommended installation procedures. The fixture shown in Figure 23 allowed the angle of the tie to be varied to produce varying L/V ratios. A spherical compression platen was used to apply load to the railhead, through a point approximately 0.50 inch in from the gage side and 0.625 inch from the top of the railhead. This location is also used to define the load application point for AREMA Chapter 30 Test 6 – Wear/Deterioration.

Load was applied at a rate of 1,000 pounds per minute until 12,000 pounds was reached or 0.5 inch of lateral railhead (gage widening) displacement was measured. The test sequence was repeated for rail angles (and corresponding L/V ratios) of zero degrees (L/V=0.0), 16.7 degrees (L/V=0.3), 21.8 degrees (L/V=0.4), 26.6 degrees (L/V=0.5), 31.0 degrees (L/V=0.6), and 45.0 degrees (L/V=1.0. The following channels were recorded throughout loading:

1. Applied resultant load

2. Resultant displacement at railhead (in-line actuator LVDT)

3. Lateral railhead displacement – right side

4. Lateral railhead displacement – left side

5. Lateral rail base displacement – right side

6. Lateral rail base displacement – left side

7. Field side rail vertical displacement – right side

8. Field side rail vertical displacement – left side

9. Gage side rail vertical displacement – right side

10. Gage side rail vertical displacement – left side

3.5.2 Results

Figure 24 through Figure 29 show the field side rail vertical displacement and railhead lateral (gage widening) displacements for the various L/V ratios. The figures are presented in order of increasing L/V ratio. Two graphs (one for Uniform and the other for Triangular—side by side for Figure 24 through Figure 29).
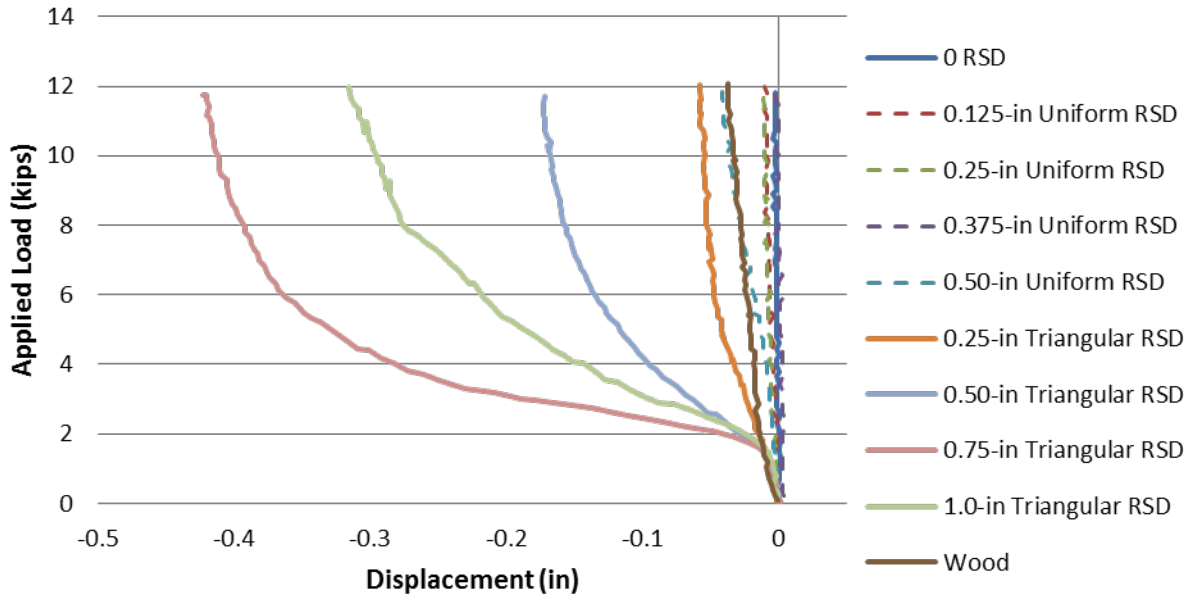
Figure 24. Field Side Vertical Displacement vs. Load for Zero L/V Ratio
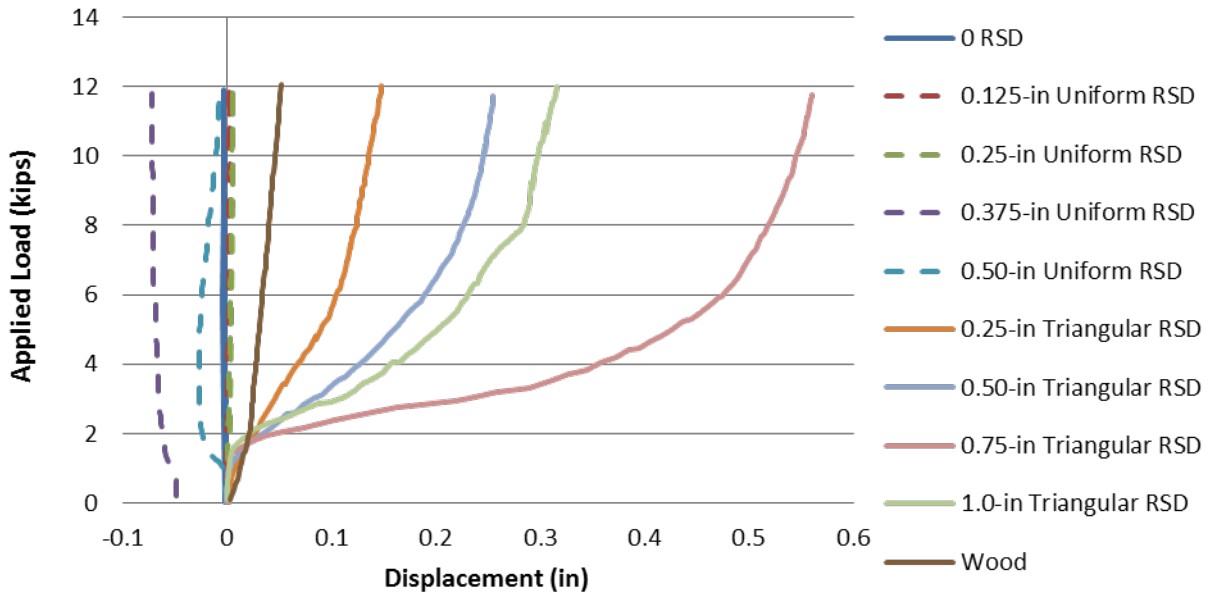
Figure 25. Lateral Gage Displacement vs. Load for Zero L/V Ratio
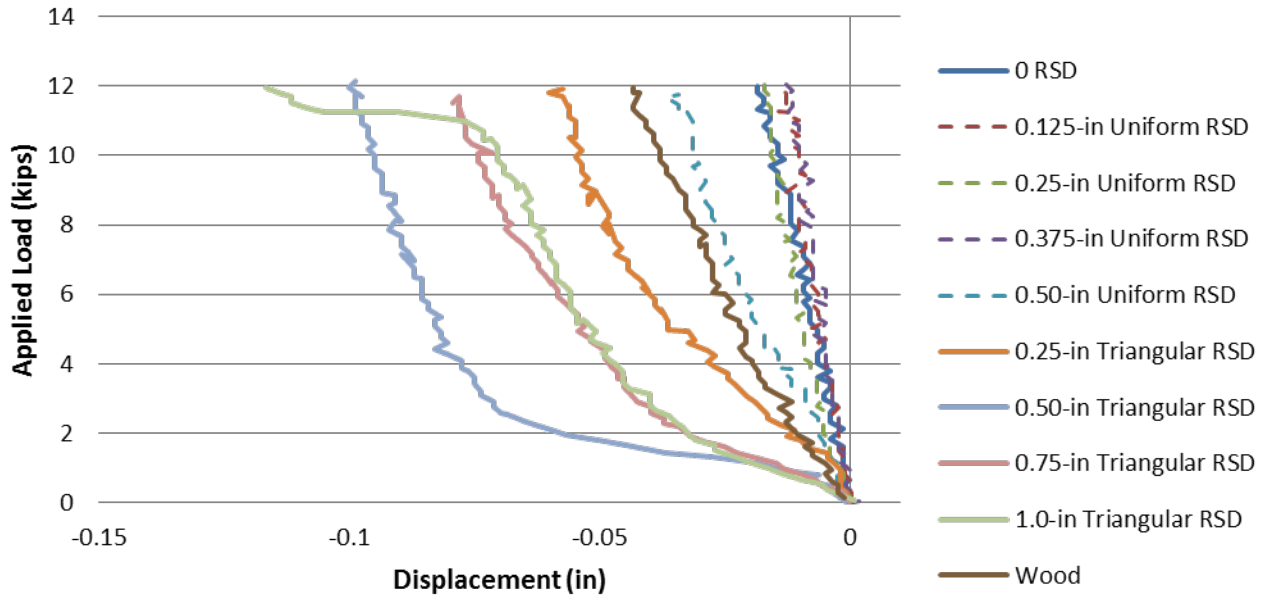
Figure 26. Field Side Vertical Displacement vs. Load for 0.5 L/V Ratio
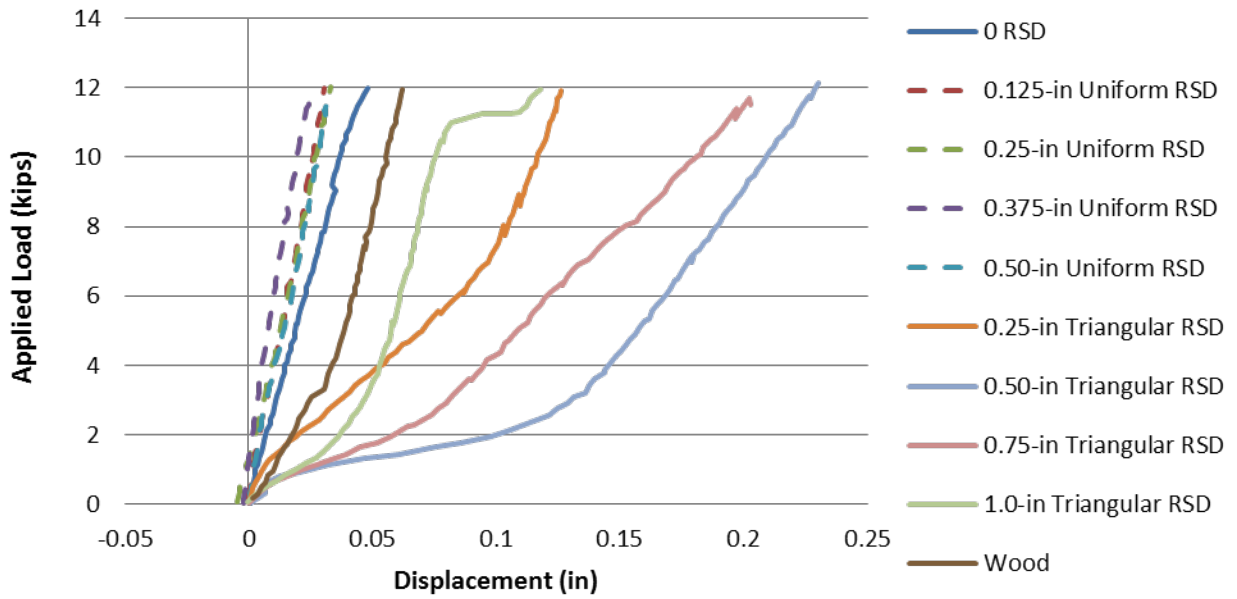
Figure 27. Lateral Gage Displacement vs. Load for 0.5 L/V Ratio
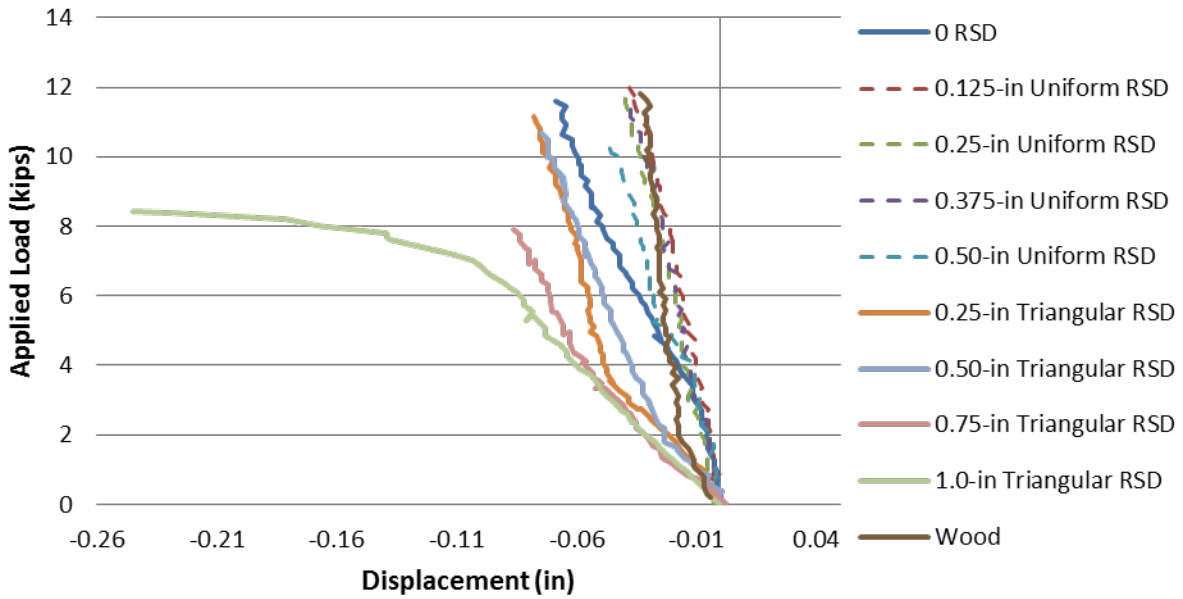
Figure 28. Field Side Displacement vs. Load for 1.0 L/V Ratio
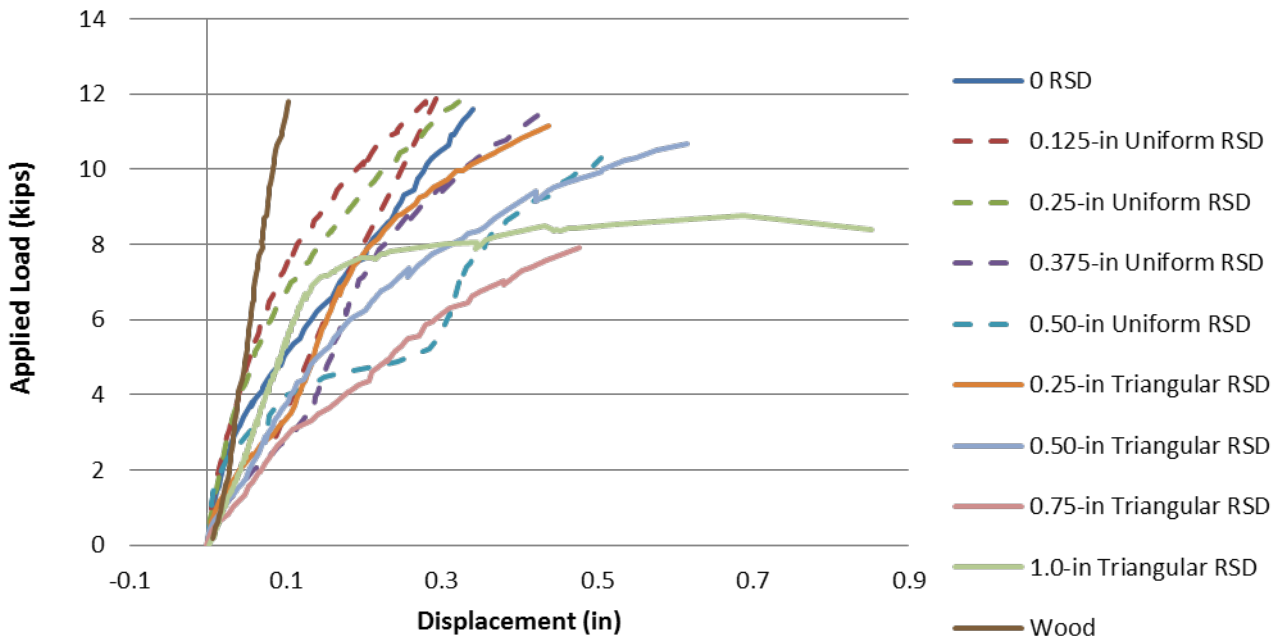
Figure 29. Lateral Gage Displacement vs. Load for 1.0 L/V Ratio

Figure 30 through Figure 33 display lateral railhead and vertical field side displacement for the various RSD conditions.
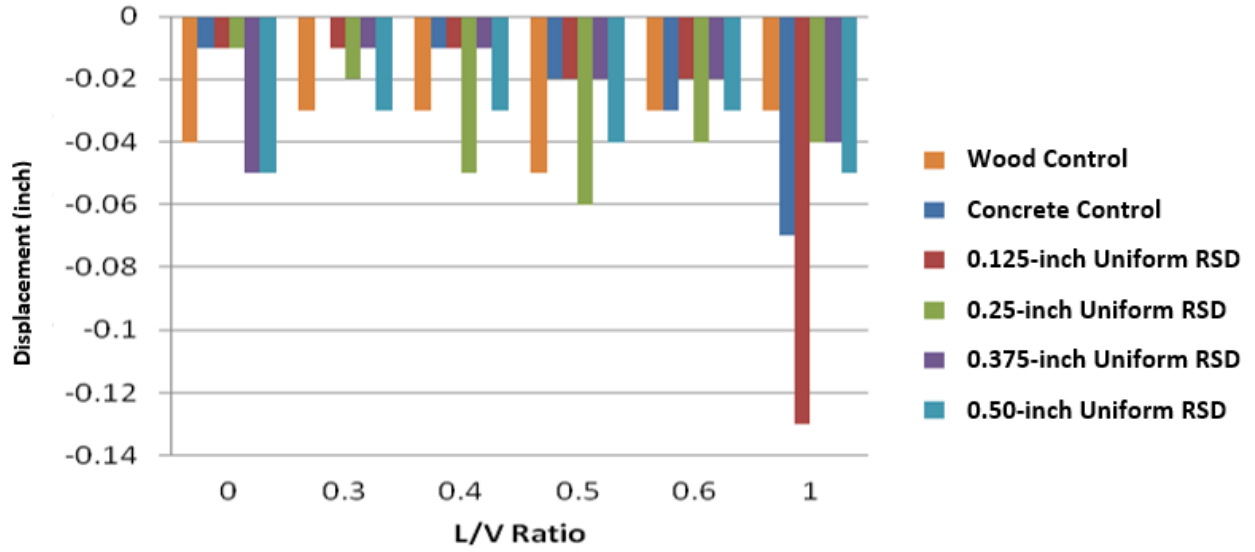
Figure 30. Vertical Field Displacement for Uniform RSD Conditions
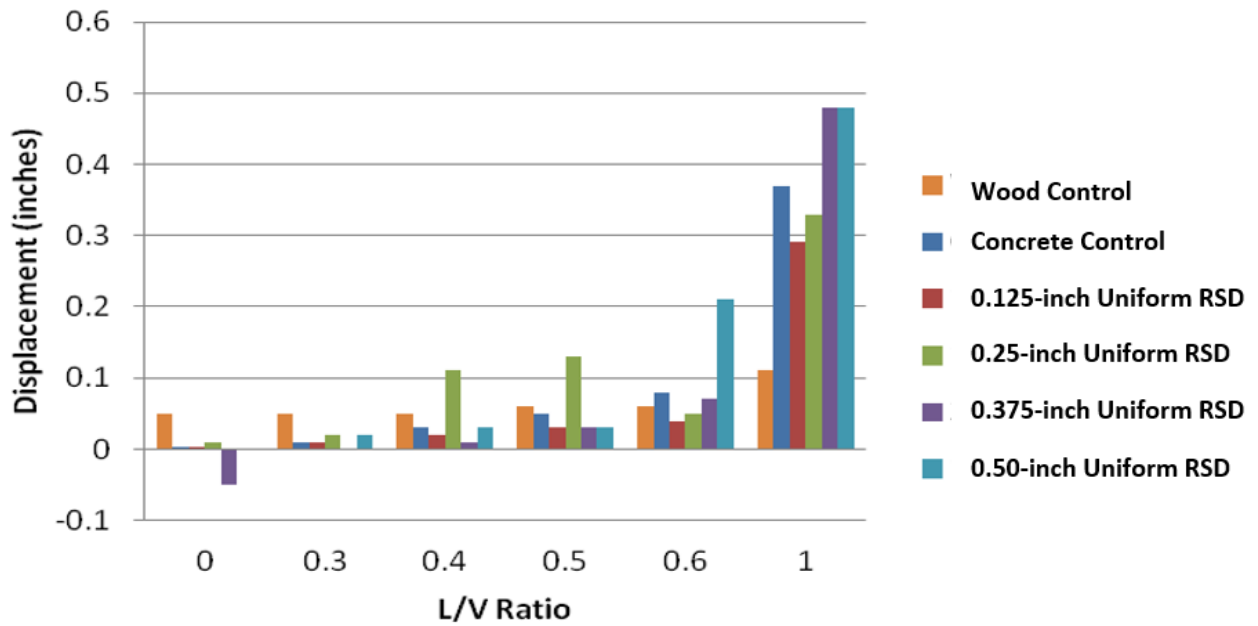
Figure 31. Lateral Railhead Displacement for Uniform RSD Conditions
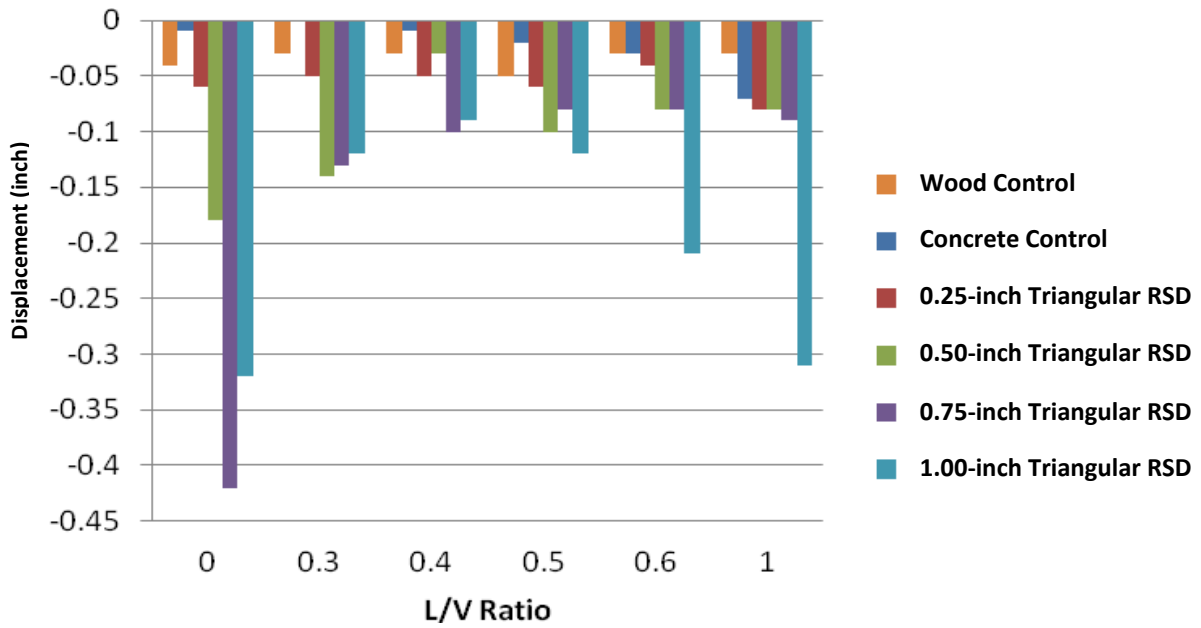
Figure 32. Vertical Field Side Displacement for Triangular RSD Conditions
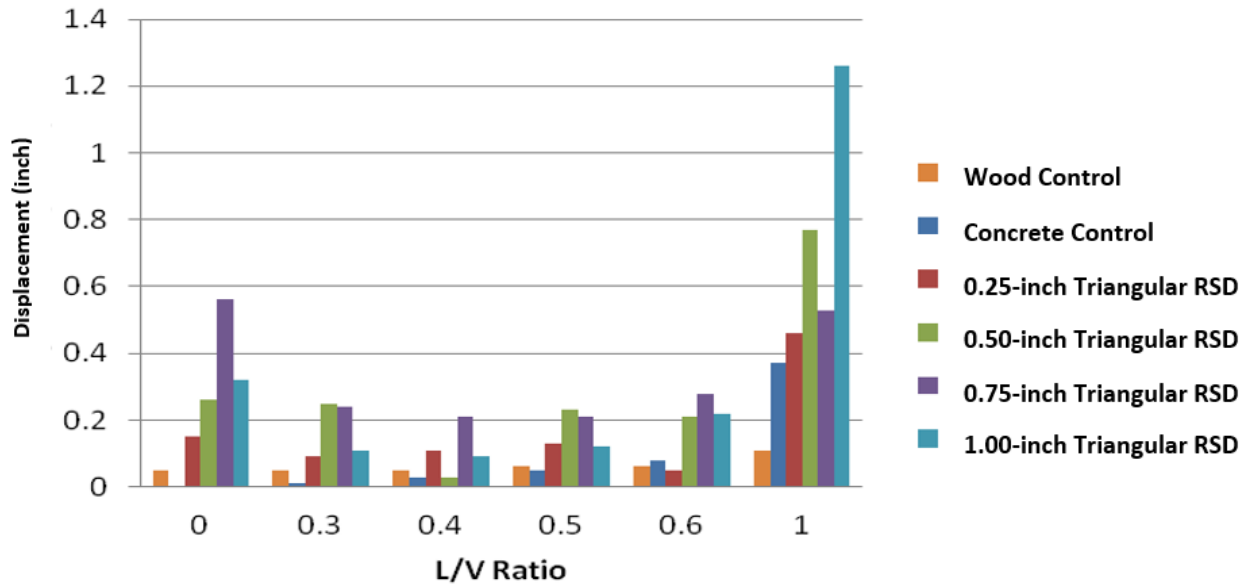
Figure 33. Lateral Railhead Displacement for Triangular RSD Conditions

Table 2 and Table 3 displays the maximum vertical field side and lateral railhead displacements, respectively, for each RSD configuration tested.

Table 2. Vertical Field Side Displacement for Varying L/V Ratios

Configuration	L/V Ratio					
	0	0.3	0.4	0.5	0.6	1
Zero RSD	**-0.01**	**0.00**	**-0.01**	**-0.02**	**-0.03**	**-0.07**
0.125-inch uniform RSD	-0.01	-0.01	-0.01	-0.02	-0.02	-0.13
0.25-inch uniform RSD	-0.01	-0.02	-0.05	-0.06	-0.04	-0.04
0.375-inch uniform RSD	-0.05	-0.01	-0.01	-0.02	-0.02	-0.04
0.50-inch uniform RSD	-0.05	-0.03	-0.03	-0.04	-0.03	-0.05
0.25-inch triangular RSD	-0.06	-0.05	-0.05	-0.06	-0.04	-0.08
0.50-inch triangular RSD	-0.18	-0.14	-0.03	-0.10	-0.08	-0.08
0.75-inch triangular RSD	-0.42	-0.13	-0.10	-0.08	-0.08	-0.09
1.0-inch triangular RSD	-0.32	-0.12	-0.09	-0.12	-0.21	-0.31
Wood	-0.04	-0.03	-0.03	-0.05	-0.03	-0.03

Table 3. Lateral Railhead Displacement for Varying L/V Ratios

Configuration	L/V Ratio					
	0	0.3	0.4	0.5	0.6	1
Zero RSD	0.001	0.01	0.03	0.05	0.08	0.37
0.125-inch uniform RSD	0.004	0.01	0.02	0.03	0.04	0.29
0.25-inch uniform RSD	0.01	0.02	0.11	0.13	0.05	0.33
0.375-inch uniform RSD	-0.05	0.00	0.01	0.03	0.07	0.48
0.50-inch uniform RSD	0.00	0.02	0.03	0.03	0.21	0.48
0.25-inch triangular RSD	0.15	0.09	0.11	0.13	0.05	0.46
0.50-inch triangular RSD	0.26	0.25	0.03	0.23	0.21	0.77
0.75-inch triangular RSD	0.56	0.24	0.21	0.21	0.28	0.53
1.0-inch triangular RSD	0.32	0.11	0.09	0.12	0.22	1.26
Wood	0.05	0.05	0.05	0.06	0.06	0.11

As expected, triangular RSD generated higher field side vertical displacements and railhead lateral displacements than similar magnitudes of uniform RSD. As triangular RSD depth was increased, higher field side vertical displacements were observed. The effect of uniform RSD depth on vertical field side displacements or lateral railhead displacements was less apparent. Results show that the wood tie sample behaved similarly to the uniform RSD cases except under the highest L/V ratio of 1.0.

The gage side fastener failed for the 1-inch triangular RSD tie section under the 1.0 L/V ratio case. This resulted in the large field side vertical and railhead lateral displacements that were observed. The 1-inch triangular RSD tie generally showed less field side vertical and railhead lateral displacement than some of the less severe triangular RSD samples, namely the 0.75-inch and 0.5-inch triangular RSD cases. This result was unexpected. One of the compliance tests was

repeated to improve understanding of the results. The authors believe the initial position of the rail before loading (i.e., being seated further into the RSD profile) and interference with the rail pad could have contributed to the lower deflections observed. This could explain why measured displacements do not consistently trend higher with increased RSD depths.

Observations made throughout testing suggest that the initial position of the rail plays a key role in how it will behave when loaded. The tests described below were conducted to better understand this relationship.

3.5.3 Effects of Initial Rail Position

To demonstrate the effect that initial rail position was having on the system, triangular and uniform RSD test ties were set up again with two different pad conditions, one simulating a deteriorated pad, and a new pad, as was used throughout laboratory testing. Figure 34 shows these two pads.

Figure 34. Cut Pad Simulating Deterioration (left) and Uncut Pad (right)

The same lateral/vertical compliance test regime was conducted. Figure 35 shows the difference observed before (left) and after (right) loading suggests that the tie pad influenced the test results by supporting the rail over the RSD initially before loading. After the load was applied, the rail clearly seated deeper into the RSD. Since the rail was not reset after each L/V test case, the rail was likely starting in a different location each time a new test was performed. Worn or modified pads might better replicate in-situ RSD conditions. However, rail temperature and the effects of adjacent ties may also prevent the rail from fully seating in the RSD profile and thus affect the initial position of the rail before it is loaded.

Figure 35. Using a New Rail Pad, Rail Before (left) and after (right) Lateral/Vertical Compliance Test

4. In-Track Detection Testing

In-track RSD detection testing was conducted on a siding track at FAST. Four RSD test zones were established with different types and magnitudes of RSD. Industry participation was solicited to test over these zones and share data and observations with TTCI's research team.

4.1 RSD Test Section Description

In order to assess various systems' ability to detect existing RSD, a test section was constructed with various types and magnitudes of artificially ground RSD test zones. The test zones were installed with conventional concrete ties and SAFELOK I fasteners. Initially, Zone 1 – Uniform RSD; Zone 2 – Light, Full Triangular; and Zone 3 – Heavy, Full Triangular were installed in 2014. Zone 4 – Heavy, Half Triangular was installed in 2015 after discussion amongst the project team about RSD conditions in revenue service. As conditions resembling half-triangular RSD have been observed, it was of interest to include this case in the test section. Figure 36 and Table 4 show the layout of the RSD test section and the types and depths of RSD in the four zones.
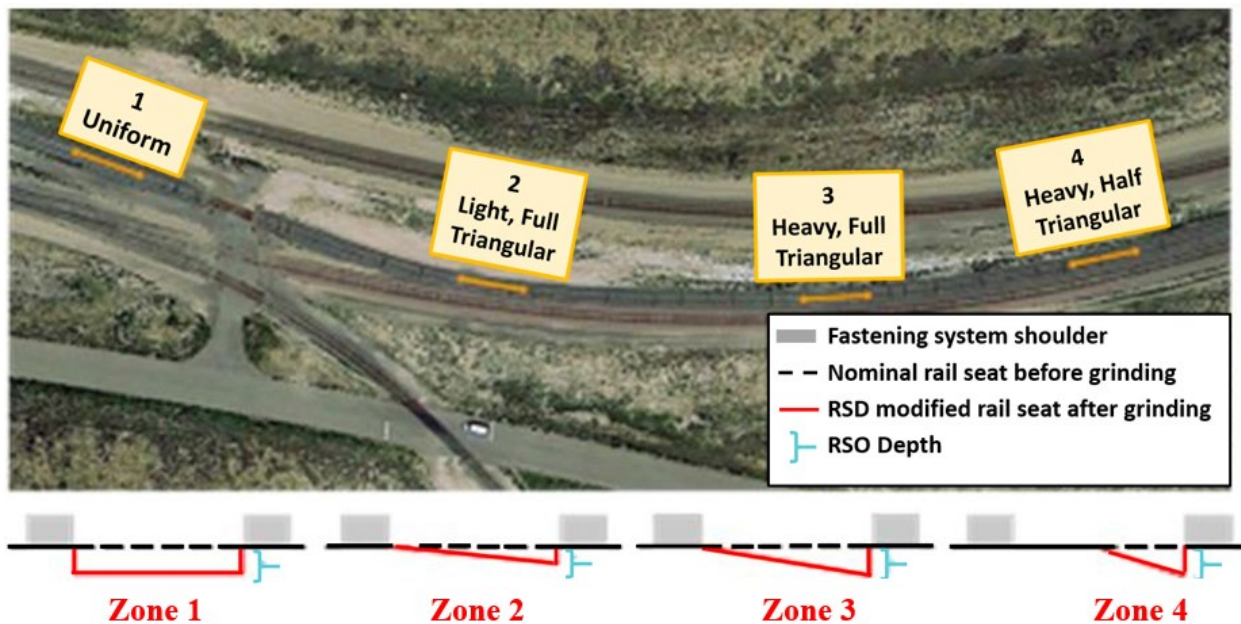
Figure 36. Layout of the Four RSD Zones Installed in the Test Section

Table 4. RSD Depth Ground into Each of the 20 Ties in Each RSD Zone

Zone Tie No.	Zone 1 – Uniform (inch)	Zone 2 – Light, Full Triangular (inch)	Zone 3 – Heavy, Half Triangular (inch)	Zone 4 – Heavy, Half Triangular (inch)
1	0.125	0.125	0.125	0.125
2	0.125	0.125	0.250	0.125
3	0.125	0.125	0.375	0.250
4	0.125	0.250	0.500	0.250
5	0.125	0.250	0.500	0.375
6	0.250	0.250	0.625	0.375
7	0.250	0.375	0.625	0.500
8	0.250	0.375	0.750	0.500
9	0.250	0.375	0.750	0.500
10	0.250	0.375	0.750	0.500
11	0.250	0.375	0.750	0.500
12	0.250	0.375	0.750	0.500
13	0.250	0.375	0.750	0.500
14	0.250	0.375	0.625	0.500
15	0.250	0.250	0.625	0.375
16	0.125	0.250	0.500	0.375
17	0.125	0.250	0.500	0.250
18	0.125	0.125	0.375	0.250
19	0.125	0.125	0.250	0.125
20	0.125	0.125	0.125	0.125

The test section was located on a minimally used siding that included tangent track and a curve of approximately 4 degrees. The uniform RSD zone (Zone 1) was located on a tangent section of track and the three triangular RSD zones were located in the body of the curve. Maximum operating speed over the test section was 20 mph; however, vehicles operated at 15 mph or less during testing.

4.2   Vehicles and Systems Tested

Various track inspection vendors were contacted at the outset of the study to solicit participation, and they were offered the opportunity to trial their respective inspection systems over the test zones. Test engineers provided basic information as to the purpose of the study and the type and magnitude of RSD that was installed. No information pertaining to specific locations of RSD ties or where particular zones were located was provided.

Table 5 shows a matrix of the inspection systems that were tested over the RSD zone. Each system is categorized by its respective capabilities and data types that are produced.

Table 5. Matrix of Systems Tested Over the RSD Test Section and Their Respective Track Inspection Capabilities

Category and Measurement		Vehicle							
		TLV*	T-18*	LTLF	Holland TrackSTAR®	T-16*	UPRR EC-5	NxGEN*	L-Kopia
Track Geometry	Surface	X	X		X	X	X	X	
	Alignment	X	X		X	X	X	X	
	Gage	X	X		X	X	X	X	
Rail	Cant		X		X	X	X	X	
	Rail Profile		X		X	X	X	X	
GRMS	Unloaded Gage	X	X	X	X				
	Loaded Gage	X	X	X	X				
	Delta Gage	X	X	X	X				
Non Load-based	Camera/ Machine Vision							X	
	Laser								X

Zone 4 - Half Triangular RSD was inspected after added in 2015

4.2.1 GRMS Testing

The presence of RSD inherently changes the surface that the rail and rail pad contact when loaded. Additionally, the deterioration of the rail seat can reduce the toe load of the fastening system. Vehicles or devices that apply a gage widening load to the rail have the possibility of detecting these changes in rail support conditions through wider loaded-gage measurements. GRMS vehicles apply an in-motion gage widening load to the track through a deployable wheelset. This independent wheelset acts as the gage spreading actuator. Vertical load and lateral load are typically applied at the same time.

Historically, various GRMS vehicles have been used to provide an assessment of track strength. The loads that these vehicles apply to perform this assessment is not standardized. GRMS systems typically output unloaded track gage, loaded track gage, and delta gage, or the difference between the loaded and unloaded gage channels. Additionally, PLG24, a parameter defined in FRA's Title 49 Code of Federal Regulations Part 213, Track Safety Standards [6], can be calculated. The calculation of PLG24 in practice is an attempt to normalize the outputs from varying load magnitudes and L/V ratios.

Three GRMS vehicles completed inspections over the RSD zones. The AAR's Track Loading Vehicle (TLV) applied wheel loads (at each rail) of 33 kips vertical and 18 kips lateral. The FRA's T-18 vehicle performed multiple runs at various L/V ratios. For the purposes of this report, a typical run of 18-kip vertical and 12-kip lateral, as well as a more severe case of 16-kip vertical and 18-kip lateral wheel loads, are reported. Lastly, Holland's TrackSTAR® testing vehicle inspected with wheel loads of 15-kip vertical and 9-kip lateral— a typical set of

parameters for Class I railroad inspections. Figure 37 shows the three GRMS vehicles and the loads that they apply.

Figure 38 compares the relative displacement of the rail head between the unloaded condition (Figure 38a) and at the moment the TLV's load axle, applying 33-kip vertical and 18-kip lateral loading, was directly over Tie 10 of Zone 3 or the heavy triangular RSD zone (Figure 38b).
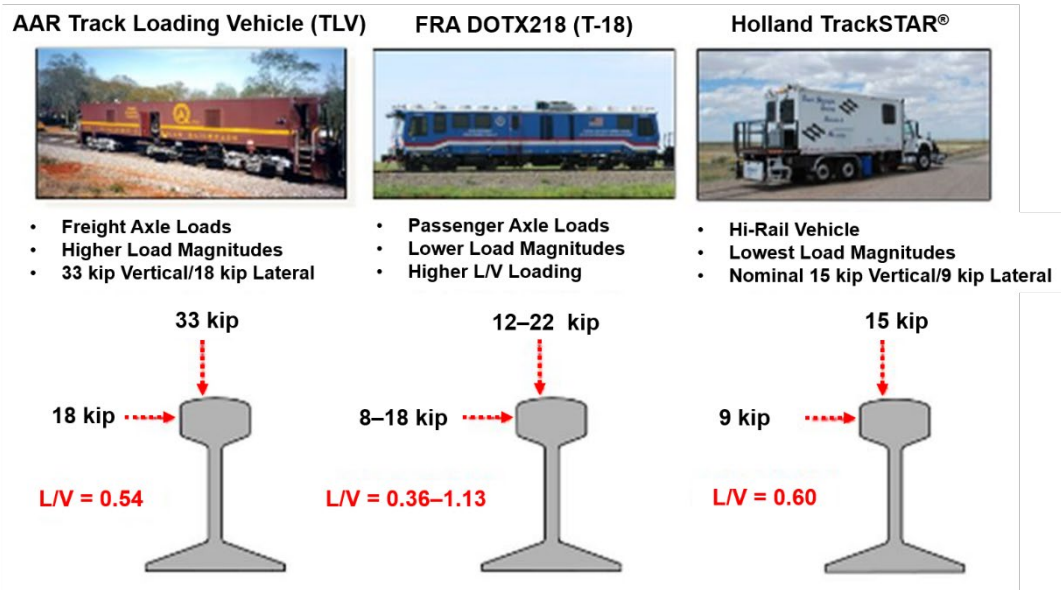
Figure 37. Three GRMS Systems Tested and Applied Load Magnitudes and L/V Ratios
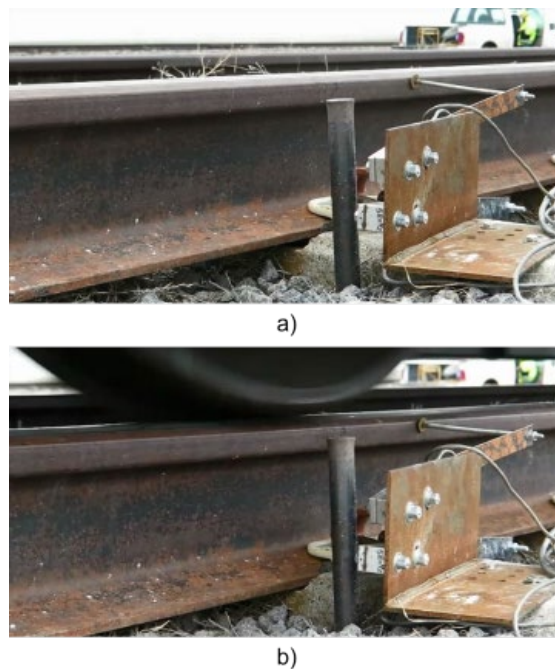
Figure 38. TLV GRMS Testing over Tie 10 of Zone 3 (0.75-inch Full Triangular RSD when: (a) Unloaded and (b) Loaded with 33-kip Vertical and 18-kip Lateral Wheel Load

35

Figure 39 shows the unloaded gage measurements taken from the three GRMS systems tested. The Holland TrackSTAR vehicle tested before the addition of Zone 4. Figure 40 shows the loaded gage measurements taken from the three GRMS systems tested.
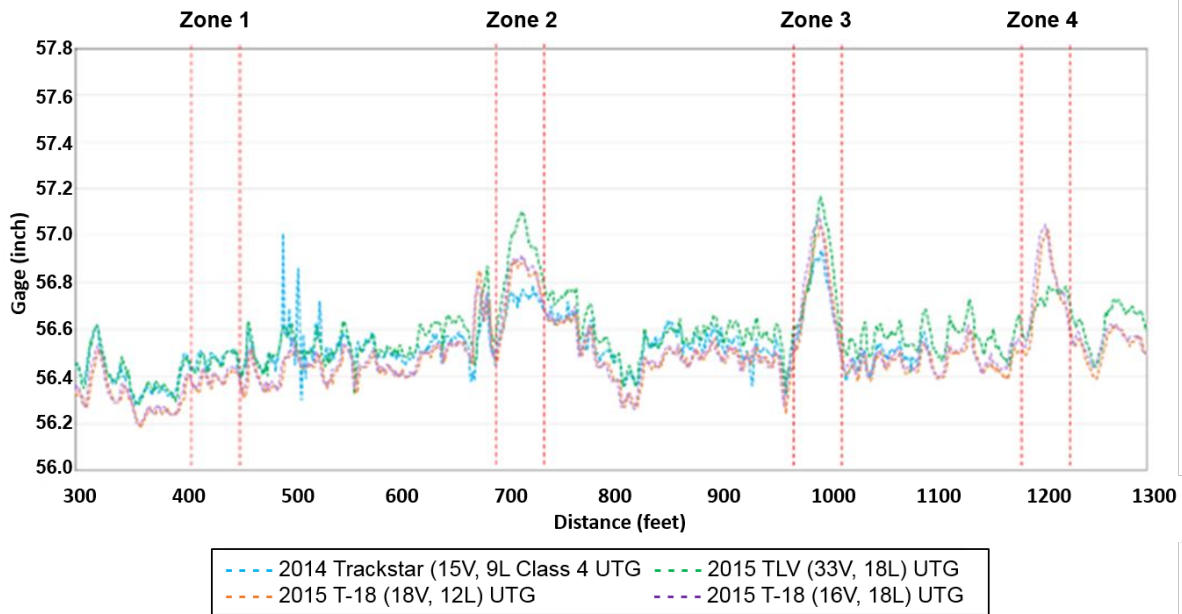
Figure 39. Unloaded Track Gage (UTG) Measurements from the Three GRMS Vehicles Tested with Varying Load Magnitudes and L/V Ratios
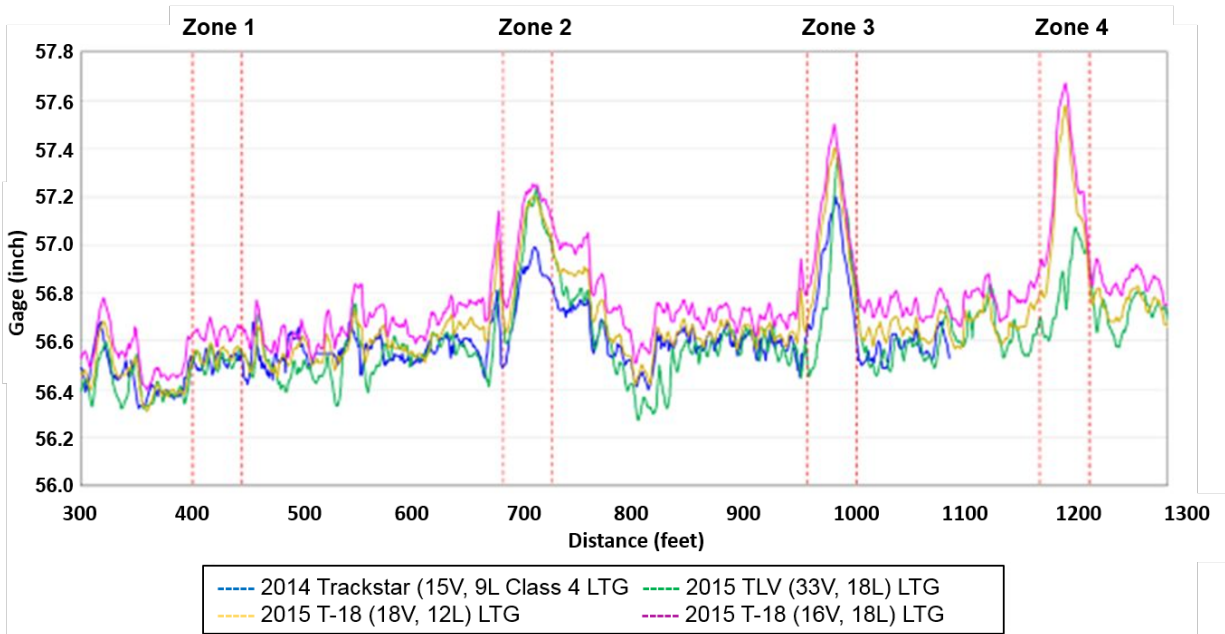
Figure 40. Loaded Track Gage (LTG) Measurements from the Three GRMS Vehicles Tested with Varying Load Magnitudes and L/V Ratios

The TLV, while not applying the highest L/V ratio of loading, produced magnitudes of gage widening similar to the two T-18 runs (with higher L/V ratios) shown. The TrackSTAR vehicle appeared to produce the lowest amount of gage widening of the test cases. It should be noted that results from the loaded gage channel of the TrackSTAR test and the unloaded gage channel of the TLV were similar likely due to the much higher static axle loads of the TLV. Higher vertical loads appear to better "seat" the rail into full triangular RSD and subsequently cause gage widening. The higher vertical loads (combined with the relatively low L/V of 0.55) of the TLV however, produced less gage widening in the half triangular test zone relative to higher L/V runs. These results suggest that higher vertical loads as well as higher L/V ratios should be considered depending on the type and magnitude of RSD that may be present.

Additionally, the T-18 was used to record loaded high rail cant through the test zones. Figure 41 shows the loaded high rail cant measurements taken from three different T-18 GRMS runs at three different load magnitudes and L/V ratios.
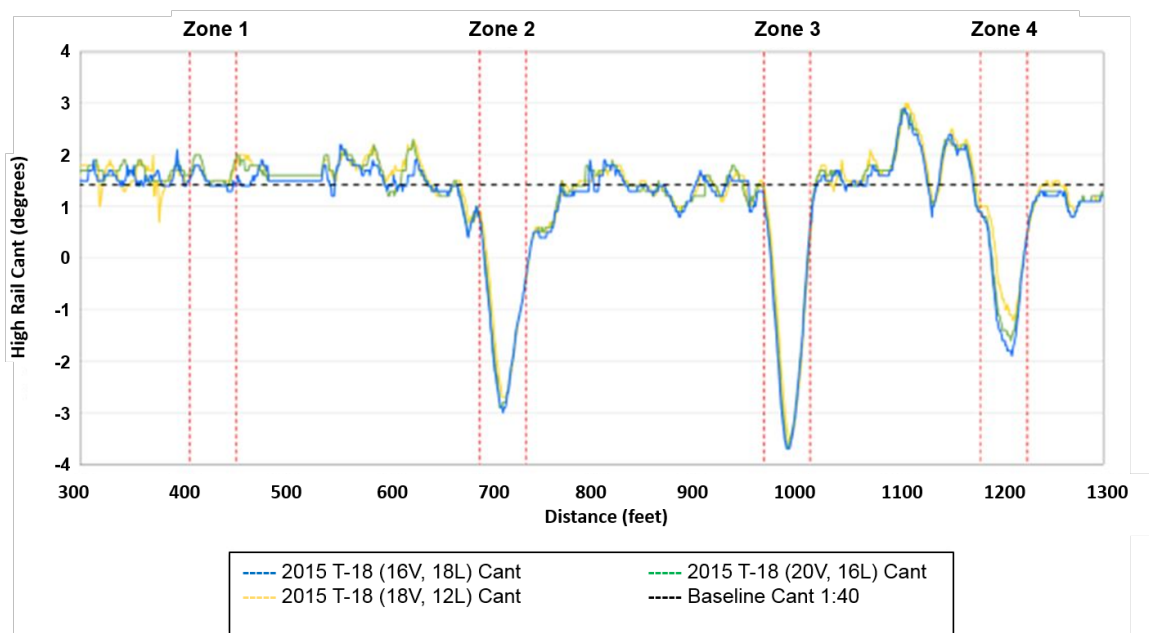
Figure 41. Loaded Cant Measurements from T-18 GRMS Runs at Three Different Load Magnitudes and L/V Ratios

It is apparent that various load magnitudes and L/V ratios used during testing did not have a significant impact on the loaded cant measurements recorded in Zones 1, 2, or 3. Zone 4 appears to show a slight increase in loaded cant for the higher L/V ratio case (16-kip vertical and 18-kip lateral). Rail rotation (cant) is not measurably affected by loads at the magnitudes that were applied for uniform RSD, and even the lower magnitudes of loads were sufficient to fully rotate and seat the rail within the levels of RSD in Zones 2 and 3.

4.2.2 Track Geometry Testing

In addition to the GRMS systems tested, the T-18, Holland's TrackSTAR, NxGen Rail Services' NxTrack™, Union Pacific Railroad's EC-5, and FRA's T-16 track geometry cars measured conventional track geometry (gage, surface, and alignment) through the RSD test zones. The

gage channel, or unloaded gage channel on the GRMS vehicles were aligned and analyzed as potential indicators of RSD. Figure 42 shows the gage channel for a selection of the track geometry systems that were tested.
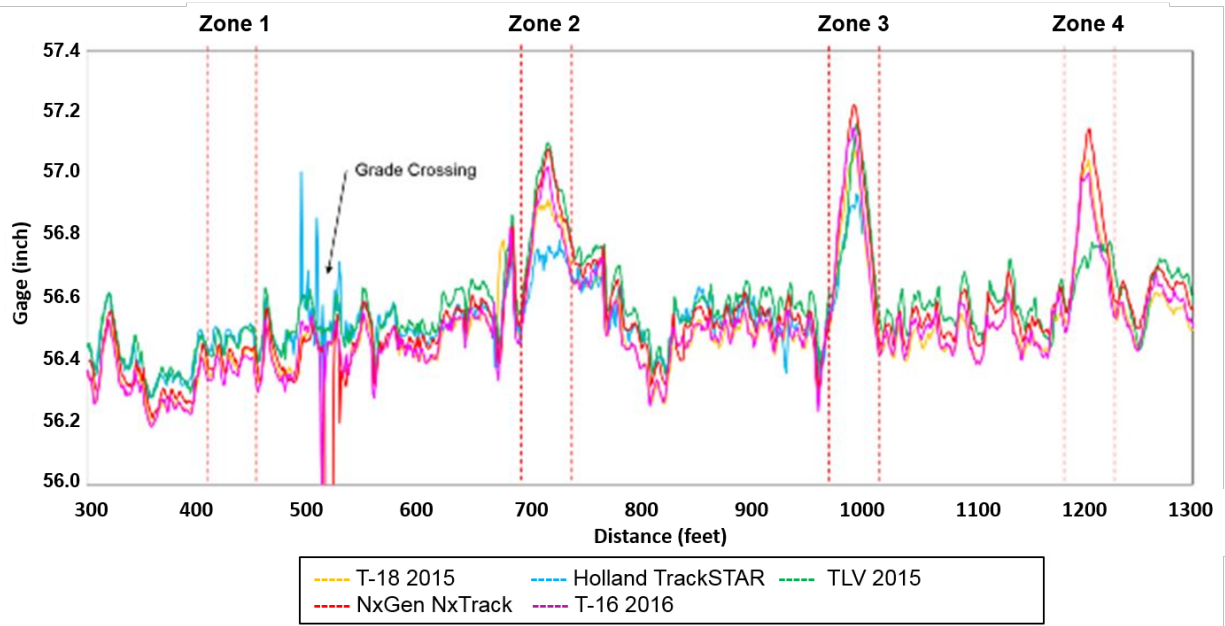
Figure 42. Track Gage as Measured by Five Different Track Geometry Vehicles that Tested Over the RSD Zones

Primarily, the track geometry systems could detect the triangular RSD zones (Zones 2, 3, and 4) as slightly wider unloaded gage (similar to the GRMS systems); however, they were not able to indicate the uniform RSD zones. The lightest track geometry system tested, the TrackSTAR, appears to have measured lower unloaded gage, likely because of its lower axle loads. Note that the TrackSTAR did not test over Zone 4, as it was added after this testing was conducted.

Figure 43 shows the unloaded gage channel overlaid against the unloaded cant channel from T-16 testing in 2016. It shows the direct relationship between the unloaded cant and unloaded gage that were recorded (identified each zone in plot below in Figure 43). Note that the T-16 test run for the data in Figure 43 was made in reverse.
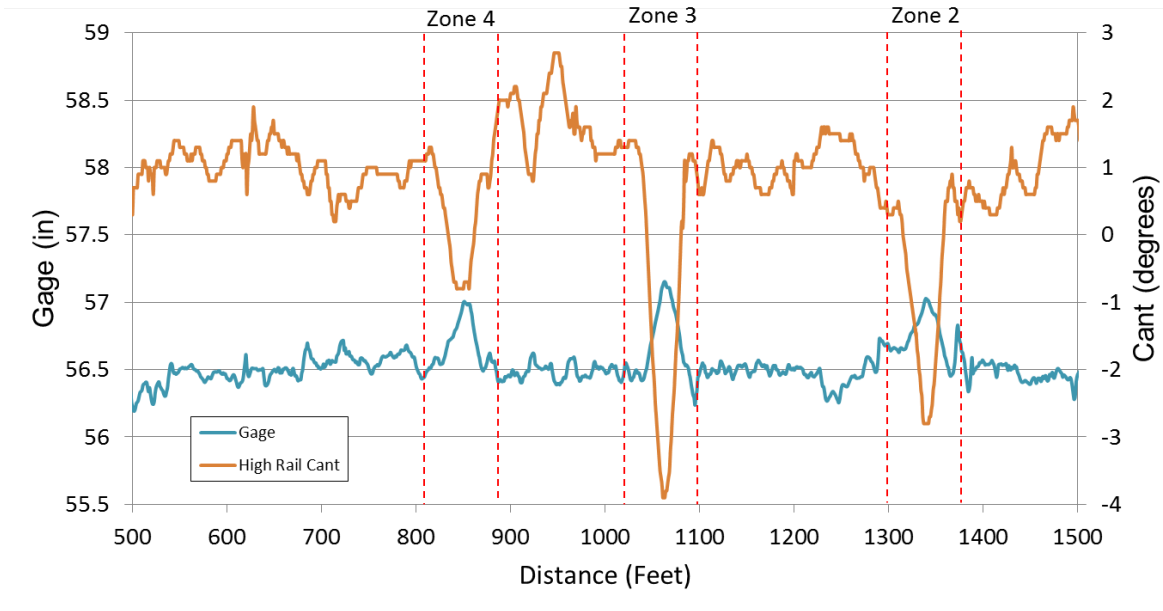
Figure 43. Track Gage Overlaid against Measured High Rail Cant by the T-16 in the Three Triangular RSD Zones

4.2.3 Other Non-Load-Based Inspection Systems

In addition to their track geometry measurement system, NxGen was provided the opportunity to use their machine vision-based inspection system to inspect the RSD zones during the same test runs. Figure 44 shows the NxTrack car during testing. Figure 45 shows three images from the system's video for an inspection run over the RSD zones. Figure 45c shows a slightly oblique angle of the high rail, field side fastener on Tie 10 of Zone 3, the Heavy, Full Triangular RSD. This camera angle is typically used by the system to inspect joint bars. However, it is evident from this image that the rail is sitting farther into the rail seat than would be typical for a non-RSD affected rail seat (note the top of the rail base flush with the concrete tie surface). These images and other track geometry data collected during testing may be used by NxGen for development of an image processing algorithm potentially capable of sensing RSD during a typical track inspection.

39

Figure 44. NxGen and NxTrack Track Geometry and Machine Vision Vehicle
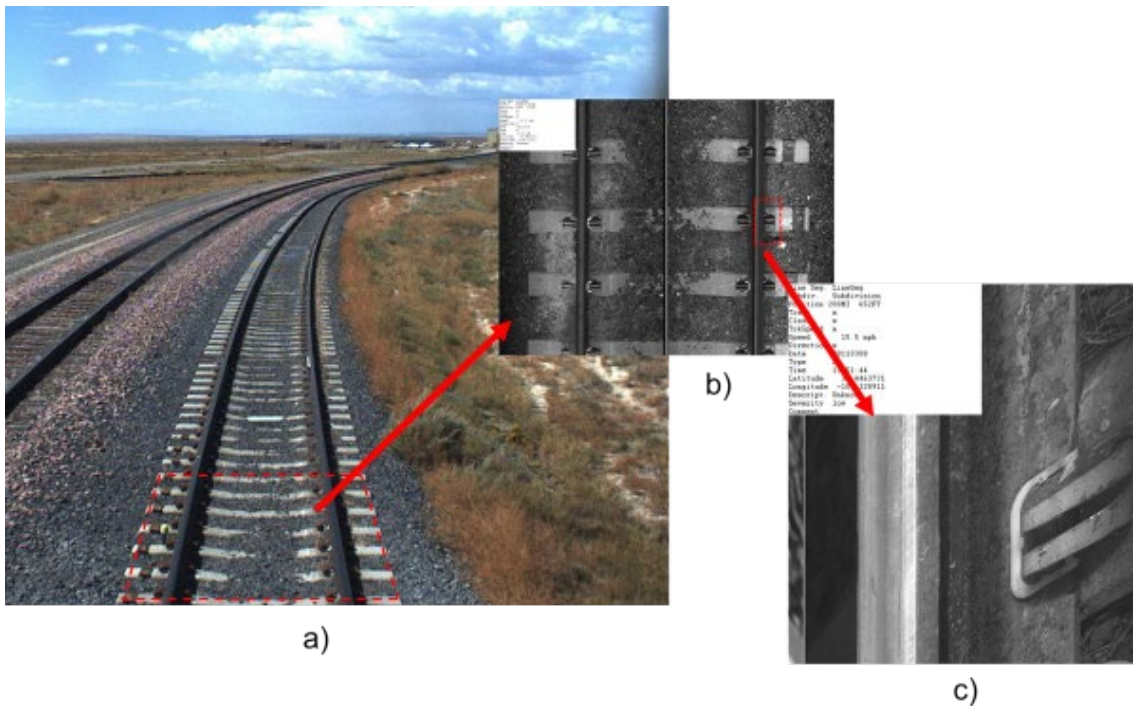
Figure 45. Images from Captured Video During NxGen Inspection over RSD Zones: (a) View from Back of Test Car, (b) Overhead View of Left (low) and Right (high) Rail, and (c) Detailed Image of High Rail Field Side of Rail Seat on Tie 10 of Zone 3 (0.75-inch Full Triangular RSD) Showing Rail Seated into RSD

L-Kopia, a company offering systems for laser-based clearance measurements was provided the opportunity to inspect over the RSD test zones. Without a history of tie or fastening system inspection, the vendor was provided access to the RSD zones to trial any new or untried

40

techniques. Data from this testing was unavailable for analysis by TTCI, and discussions with the vendor concluded that no data was generated that would have detected RSD.

The Georgetown Rail Aurora® inspection system, a track inspection system currently in use in the industry was offered the opportunity to participate but was not available for inclusion in the test program. Georgetown may elect to test over the RSD zones in the future.

4.2.4 Additional Testing over the RSD Test Section

In addition to detection and inspection testing conducted under this project, additional studies have used the RSD test section on related research projects. Greve, et al. (2015) utilized Zones 1 through 3 to conduct measurements of rail seat pressures as various applied load magnitudes and L/V ratios for the different types and depths of RSD [7].

ENSCO, the contracted operator of the FRA test vehicles used in this study (T-16 and T-18) has also used the test section to conduct studies with the T-18 vehicle to better understand the sensitivity of loaded gage and loaded cant measurements to RSD type and depth. A report on this study is forthcoming.

The test zones will be available to other vendors for testing through most of 2017.

5. Conclusion, Discussion, and Recommendations

Laboratory and in-track testing was conducted as a part of this study to better understand the effect of various types and magnitudes of RSD on rail behavior and how this behavior may impact RSD detection.

Ties with and without preexisting RSD were installed on the HTL at FAST and accumulated 375 MGT of heavy axle load tonnage in a high degree curve operated at overbalance speed. RSD was not observed to develop on either the non-deteriorated ties or the ties with preexisting RSD. These observations agree with previous concrete tie tests at FAST where RSD is not a documented failure mode. Results from this portion of the study suggest that a moister environment may be necessary to induce and develop RSD; this appears to be a key variable missing in the FAST environment. Additionally, despite documented higher rail seat stresses [8], the presence of preexisting RSD did not contribute to any additional RSD development in this test. Results augment support for an abrasive mechanism of RSD, often called rail seat abrasion or RSA, instead of an ultimate failure or crushing mode. The rate of RSD development should be further studied to better guide inspection frequencies.

It should be noted that in recent years, Class I railroads in the United States have begun to see RSD as a failure mode mitigated through improved tie and fastener design and rail seat renewal. Conventional industry practice is to restore concrete tie and fastener performance with new rail pads and fasteners. As railroads have become more diligent about replacement of rail pads and fastening systems and the epoxy repair of rail seats, the development of RSD may be delayed or mitigated. Improved ballast maintenance practices and scheduled surfacing intervals also contribute to prolonged tie life.

Laboratory testing was first conducted to provide preliminary conclusions and guide in-track RSD detection testing. Longitudinal rail restraint, rail uplift, and lateral/vertical compliance testing was conducted on samples of ties with a variety of types and magnitudes of RSD that were artificially ground into the rail seats. Rail uplift test results confirmed that both the gage and field side fastener toe loads are reduced with increasing uniform RSD. This reduction in toe load across the rail seat is the primary contributor to reduced rail longitudinal restraint. Tests showed significantly less longitudinal rail restraint with increasing uniform RSD. Longitudinal rail restraint was less impacted by increasing magnitudes of triangular RSD since the gage side clip toe load is less affected in triangular RSD cases.

The results for lateral/vertical compliance tests showed anticipated rail behavior on ties with RSD, namely higher lateral railhead (gage widening) displacements and vertical field side displacements for higher magnitudes of triangular RSD. These results confirm what was observed during in-track GRMS inspections—that rail roll and loaded gage are the best indicators of triangular RSD. There was little practical difference between the railhead lateral displacement measurements for ties with zero RSD and those with varying magnitudes of uniform RSD. This result confirms what was observed throughout GRMS inspection testing— that the uniform RSD mode is indistinguishable from non-deteriorated track when assessing the rail roll and loaded gage channels. Uniform RSD may remain difficult to detect in track exclusively through GRMS testing. However, due to reduced toe loads, evidence of increased rail longitudinal movement may indicate the presence of uniform RSD.

In the final part of this study, industry suppliers with emerging and established technologies were solicited to conduct inspections over four artificial RSD test zones with varying types and magnitudes of RSD. Data from various track geometry, GRMS, and non-load-based systems was analyzed.

Track geometry systems generally saw the triangular RSD zones as areas of wide gage. Heavier track geometry cars that help seat the rail into the RSD profile (particularly for triangular RSD in curves) may help detect the presence of RSD in the gage data.

GRMS inspection testing conducted over the artificial RSD test zones indicated that GRMS vehicles are capable of indicating the locations of the full triangular and half triangular RSD types. None of the GRMS systems conclusively indicated RSD at the uniform RSD zone. Loaded cant measurements taken from various T-18 runs at varying load magnitudes and L/V ratios indicate the three triangular RSD zones clearly. Higher applied L/V ratios and higher load magnitudes, such as those applied by the TLV, appear to contribute to greater resolution in detecting triangular RSD.

The machine vision system and laser-based system tested could not directly indicate the presence of RSD in any of the zones. However, the data collected by these vendors during testing has been made available for development of imaging and inspection algorithms that may be able to output the presence of RSD in the future.

Lateral/vertical compliance testing in the laboratory and GRMS testing indicated the importance of the initial position of the rail before loading. During laboratory testing, it was shown that the rail may or may not fully seat into severe triangular RSD depending on the condition of the pad. All laboratory tests were conducted with a short piece of rail on a single tie. Thus, torsional resistance, the effect of adjacent ties, or rail temperature were not considered in laboratory testing. Lower torsional resistance, or warmer rail temperatures may contribute to the rail fully seating in a triangular RSD profile on the high rail of a curve. Conversely, colder temperatures or lower torsional resistance may influence the rail base in resting outside of the RSD profile. These variables may change over time and may affect the initial, unloaded position of the rail as well as how it behaves under loading. Thus, for GRMS, the initial position of the rail, such as measured in the unloaded gage and unloaded cant channels, should be considered in addition to the channels measured under loading (loaded gage and loaded cant) when inspecting for RSD.

It is also important to consider the location of the wheel-rail contact position in GRMS testing. GRMS vehicles will likely have differing wheel profiles. Additionally, rail size and rail profile will also differ depending on the track being tested. The wheel's contact with the rail (which is typically flanging during GRMS testing) results in an effective contact point, or a point through which the resultant applied load (lateral and vertical) acts. All else being equal, as this point shifts farther toward the field side of the railhead, the applied loading becomes more severe. Worn rail, particularly the gage face wear common in curves, may shift this effective contact point toward the field side of the rail and generate more severe loaded gage and rail roll results. The locations of the applied loads shown in Figure 37 are purposely not dimensioned.

This concept can also be thought of in terms of an "effective pivot point" of the rail (i.e., a point about which the rail rotates). For full triangular RSD, this point is likely closer to the gage side edge of the rail base. For half triangular RSD, this point may be located near the center of the rail seat. Higher applied L/V ratios may also affect this pivot point. The effect of GRMS wheel-rail contact position on testing results is a potential problem statement for future research.

43

The position of the rail is also important to consider for imaging or non-contact based detection systems. Since these systems are not typically loading the track significantly, imaging algorithms should be targeted to identify a gap between the rail base, rail pad, and rail seat (if the rail is not fully seated in the RSD profile) or an abnormal position of the rail base relative to a fixed location on the tie (if the rail is fully seated into the RSD profile. Ultimately, a combination of imaging-based and load-based inspection technologies may be the most optimal approach for detecting RSD. GRMS systems, and moreover track geometry systems, appear to be more robust and well developed, but have the drawback of not being able to detect uniform RSD. As imaging-based inspection technologies develop, they are likely to augment more conventional techniques to improve the rate at which RSD is identified.

6. References

1. Zeman, J. C., Edwards, J. R., Barkan, C. P. L., and Lange, D. A. "Failure mode and effect analysis of concrete ties in North America." In *Proc. of the 9th International Heavy Haul Conference*, pp. 270–278. 2009.

2. Reiff, R., Walker, R., Schreiber, P., Wilson, N., and Thompson, H. "Assessment of Rail Seat Abrasion Patterns and Environment." DOT/FRA/ORD-12/07, Department of Transportation, Federal Railroad Administration, Washington, DC, May 2012.

3. McHenry, M., Klopp, A., and Thompson Hugh. 2016. "A Dynamic Vehicle-Track Model to Study the Effects of Track Geometry and Vehicle-Track Interaction on Concrete Tie Rail Seat Load Environment." *Transportation Research Record: Journal of the Transportation Research Board*, *2545*(2545): pp. 11–19.

4. National Transportation Safety Board, Derailment of Amtrak Passenger Train No. 27, Accident No. DCA05FR010 (NTSB/RAB-06/03). October 18, 2006.

5. Marquis, B. P., Muhlanger, M., and Jeong, D. Y. "Effect of Wheel/Rail Loads on Concrete Tie Stresses and Rail Rollover." Proceedings of the *ASME 2011 Rail Transportation Division Fall Technical Conference*, American Society of Mechanical Engineers, pp. 143–150, Minnesota, MN, 2011.

6. Federal Railroad Administration. *Track and Rail and Infrastructure Integrity Compliance Manual: Volume II -, Chapter 1*, Classes 1 through 5, January 2014.

7. Greve, M. J., Dersch, M. S., Edwards, J. R., Barkan, C. P. L., Thompson, H., Sussmann, T. R., and McHenry, M. T. "Examination of the Effect of Concrete Crosstie Rail Seat Deterioration on Rail Seat Load Distribution." *Transportation Research Record: Journal of the Transportation Research Board*, *2476*(2015): 1–7.

8. McHenry, M., and LoPresti, J. "Tie and Fastener System Gage Restraint Performance at FAST." *Technology Digest*, TD-15-013, Association of American Railroads, Transportation Technology Center, Inc., Pueblo, CO, May 2015.

9. American Railway Engineering and Maintenance-of-Way Association. *Manual for Railway Engineering, Chapter 30 – Ties*, Lanham, MD, 2016.

Abbreviations and Acronyms

ACRONYMS	EXPLANATION
AREMA	American Railway Engineering Maintenance-of-Way Association
AAR	Association of American Railroads
FAST	Facility for Accelerated Service Testing
FRA	Federal Railroad Administration
GRMS	Gage Restraint Measurement System
HAL	Heavy Axle Load
HTL	High Tonnage Loop
LTG	Loaded Track Gage
L/V	Lateral/Vertical Ratio
LVDT	Linear Variable Displacement Transducer
MGT	Million Gross Tons
RSA	Rail Seat Abrasion
RSD	Rail Seat Deterioration
SRI	Strategic Research Initiative
TLV	Track Loading Vehicle
TTC	Transportation Technology Center (the site)
TTCI	Transportation Technology Center, Inc. (the company)
UPRR	Union Pacific Railroad
UTG	Unloaded Track Gage
Volpe	Volpe National Transportation Systems Center